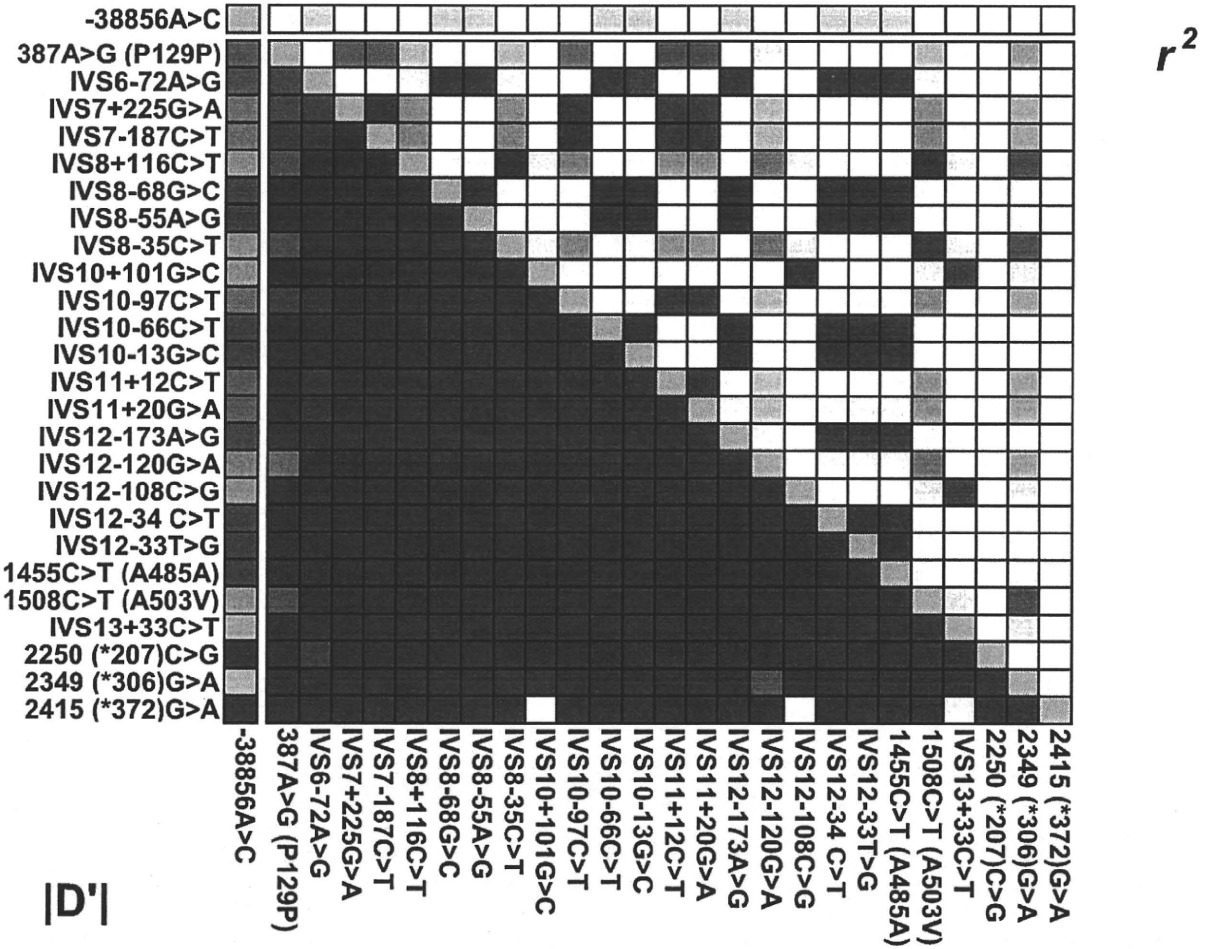
-38856A>C
387A>G (P129P)
IVS6-72A>G
IVS7+225G>A
IVS7-187C>T
IVS8+116C>T
IVS8-68G>C
IVS8-55A>G
IVS8-35C>T
IVS10+101G>C
IVS10-97C>T
IVS10-66C>T
IVS10-13G>C
IVS11+12C>T
IVS11+20G>A
IVS12-173A>G
IVS12-120G>A
IVS12-108C>G
IVS12-34 C>T
IVS12-33T>G
1455C>T (A485A)
1508C>T (A503V)
IVS13+33C>T
2250 (*207)C>G
2349 (*306)G>A
2415 (*372)G>A
|D'|
r 2

Fig. 1

Clinical Outcome of Small Cell Lung Cancer with Pericardial Effusion but without Distant Metastasis

Seiji Niho, MD, Kaoru Kubota, MD,* Kiyotaka Yoh, MD,* Koichi Goto, MD,* Hironobu Ohmatsu, MD,* Keiji Nihei, MD,† Yuichiro Ohe, MD,* and Yutaka Nishiwaki, MD**

Background: Pericardial effusion is defined as M1a in the Union Internationale Contre le Cancer seventh tumor, node, metastasis edition for lung cancer. The clinical course of small cell lung cancer (SCLC) with pericardial effusion but without distant metastasis (M1a) has not been adequately investigated.

Methods: The medical records of patients with SCLC treated at the National Cancer Center Hospital East between July 1992 and December 2007 were reviewed. During this period, 766 patients were newly diagnosed as having SCLC. Thirty-three of the 416 patients with limited disease (LD) SCLC (8%) had pericardial effusion. Seventy-nine patients with LD-SCLC (19%) had ipsilateral pleural effusion or dissemination. Of these, 16 patients had both pericardial and ipsilateral pleural effusion. We divided the 96 M1a patients into two subgroups: group A (n = 33) included patients with pericardial effusion, and group B (n = 63) included patients with ipsilateral pleural effusion or disseminated pleural nodules but without pericardial effusion.

Results: The median survival time among the patients with LD-M1a was 13.4 months (95% confidence interval: 10.7–16.6 months), and the 1-, 2-, 3-, and 5-year survival rates were 56%, 18%, 9%, and 8%, respectively. The survival of the patients with LD-M1a was intermediate between those of the patients with LD-M0 and patients with extensive disease M1b ($p < 0.0001$). The overall survival period was not statistically different between groups A and B ($p = 0.5182$). Nineteen patients in group A received chemoradiotherapy, but only two patients survived for more than 2 years (2- and 5-year survival rate: 11% both). Twenty-six patients in group B received chemoradiotherapy, and four patients survived for more than 5 years (5-year survival rate: 18%).

Conclusions: Long-term survival was achieved among patients with SCLC with pericardial effusion but without distant metastasis who successfully underwent chemoradiotherapy, although 5-year survival rate in these patients was relatively lower than in patients with SCLC with ipsilateral pleural effusion but without pericardial effusion or distant metastasis.

Divisions of *Thoracic Oncology and †Radiation Oncology, National Cancer Center Hospital East, Chiba, Japan.

Disclosure: The authors declare no conflicts of interest.

Address for correspondence: Seiji Niho, MD, Division of Thoracic Oncology, National Cancer Center Hospital East, Kashiwanoha 6-5-1, Kashiwa, Chiba 277-8577, Japan. E-mail: siniho@east.ncc.go.jp

ISSN: 1556-0864/11/0603-0001

Key Words: Small cell lung cancer, Limited disease, Pericardial effusion.

(*J Thorac Oncol.* 2011;6: 000–000)

Lung cancer is the leading cause of cancer-related deaths worldwide. Small cell lung cancer (SCLC) accounts for approximately 15% of all forms of lung cancer. Compared with non-SCLC, SCLC grows rapidly, quickly disseminates to the regional lymph nodes and distant sites, and is sensitive to chemotherapy with a response rate of 70 to 80%. The Veterans Administration Lung Study Group proposed a clinical two-stage system for SCLC that distinguishes limited disease (LD) and extensive disease (ED). LD is defined as being limited to one hemithorax, including mediastinal, contralateral hilar, and ipsilateral supraclavicular lymph nodes, whereas ED represents tumor spread beyond these regions.[1] The current standard care for LD-SCLC is a combination of chemotherapy and thoracic radiotherapy (TRT). Conversely, ED-SCLC is treated with chemotherapy alone. The original definition of LD was a tumor volume that could be encompassed by a reasonable radiotherapy plan. According to the International Association for the Study of Lung Cancer (IASLC)'s consensus report, however, the classification of LD-SCLC includes bilateral hilar or supraclavicular nodal involvement and ipsilateral pleural effusion, regardless of whether the cytological findings are positive or negative.[2] Pericardial effusion has not been defined precisely.

In 2007, the IASLC proposed a new tumor, node, metastasis (TNM) classification for lung cancer,[3–6] and the Union Internationale Contre le Cancer (UICC) seventh TNM edition has been available since 2009. According to the UICC seventh TNM edition, malignant pleural or pericardial effusion and tumor with pleural nodules are defined as M1a, leading to stage IV. An analysis of 12,620 patients with SCLC in the IASLC database demonstrated that patients who have ipsilateral pleural effusion without extrathoracic metastases (M1a) have a survival that is intermediate between stages I and III without effusion and stage IV. Nevertheless, no information regarding the presence of pericardial effusion is available in the IASLC database.[7]

Our previous retrospective analysis also demonstrated that the survival of patients with LD-SCLC with ipsilateral pleural effusion was intermediate between those of patients with LD without ipsilateral pleural effusion and patients with

ED, and long-term survival was achieved by patients with LD-SCLC who successfully underwent definitive TRT after their ipsilateral pleural effusion had disappeared after induction chemotherapy.[8] In this retrospective study, we investigated the clinical course and overall survival among patients with LD-SCLC with pericardial effusion, compared with those among patients with ED-SCLC or LD-SCLC with or without ipsilateral pleural effusion.

PATIENTS AND METHODS

In this study, LD-SCLC was defined as disease limited to one hemithorax, including mediastinal, contralateral hilar, and supraclavicular lymph nodes, ipsilateral pleural effusion, and pericardial effusion; ED-SCLC was defined as tumor spread beyond these manifestations.

We retrospectively reviewed the medical records of patients with lung cancer treated at the National Cancer Center Hospital East between July 1992 and December 2007.

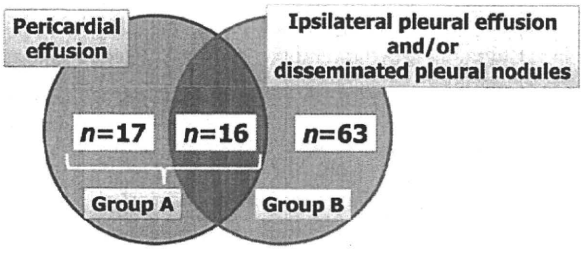

FIGURE 1. Patients with small cell lung cancer with M1a. Group A included patients with pericardial effusion, and group B included patients with ipsilateral pleural effusion or disseminated pleural nodules, but without pericardial effusion.

During this period, 766 patients were newly diagnosed as having SCLC. Four hundred sixteen patients were diagnosed as having LD-SCLC and 350 were diagnosed as having ED-SCLC using conventional staging procedures, including a medical history and physical examination, chest radiography, computed tomography (CT) scan of the chest, CT scan or ultrasound of the abdomen, bone scan, and CT scan or magnetic resonance imaging of the brain. Thirty-three of the 416 patients with LD-SCLC (8%, 95% confidence interval [CI]: 6–11%) had pericardial effusion and were included in this study. Seventy-nine of the 416 patients with LD-SCLC (19%, 95% CI: 15–23%) had ipsilateral pleural effusion or dissemination. Four patients had a disseminated mass without pleural effusion detected using CT scan. Sixteen patients with LD-SCLC had both pericardial and ipsilateral pleural effusion. Therefore, 63 patients with LD-SCLC had ipsilateral pleural effusion or dissemination without pericardial effusion. We divided the 96 M1a patients into two subgroups: group A included patients with pericardial effusion, and group B included patients without pericardial effusion. Group B patients had ipsilateral pleural effusion or disseminated pleural nodules (Figure 1).

The overall survival time was defined as the interval between the start of treatment and death or the final follow-up visit. The median overall survival time was estimated using the Kaplan-Meier analysis method.[9] Survival data were compared among the groups using a log-rank test. This study was approved by an institutional review board.

RESULTS

The patient characteristics are listed in Table 1. Eighty-three percent of the patients were male, and 81% had a performance status of 0 or 1. Fifty-four percent of the patients

TABLE 1. Patient Characteristics

	ED-SCLC (M1b)	LD-SCLC with Pericardial Effusion (M1a) (Group A)	LD-SCLC with Ipsilateral Pleural Effusion but without Pericardial Effusion (M1a) (Group B)	LD-SCLC (M0)
No. of patients	350	33	63	320
Sex				
Male	291	29	50	262
Female	59	4	13	58
Age (yr)				
Median	66	67	68	66
Range	28–85	37–82	46–83	22–87
Performance status				
0	22	0	4	108
1	224	25	47	190
2	63	6	9	15
3–4	41	2	3	7
Treatment delivered				
Chemotherapy	316	14	36	50
Chemoradiotherapy	25	19	26	224
Surgery + chemotherapy	0	0	0	33
Surgery alone	0	0	0	10
Best supportive care	9	0	1	3

LD, limited disease; SCLC, small cell lung cancer; ED, extensive disease.

TABLE 2. Timing of Thoracic Radiotherapy in Patients with M1a Small Cell Lung Cancer

Timing of Thoracic Radiotherapy	LD-SCLC with Pericardial Effusion (M1a) (Group A, $n = 19$)	LD-SCLC with Ipsilateral Pleural Effusion but without Pericardial Effusion (M1a) (Group B, $n = 26$)
Concurrently with the first course of chemotherapy	0	3
Concurrently with the second course of chemotherapy	0	4
Concurrently with the third course of chemotherapy	8	5
Concurrently with the fourth course of chemotherapy	4	0
Sequentially after chemotherapy	7	14

LD, limited disease; SCLC, small cell lung cancer.

received chemotherapy, and 38% received chemoradiotherapy. Six percent of the patients underwent surgical resection with or without adjuvant chemotherapy. Among the 96 patients with LD-M1a, all but one patient received chemotherapy ($n = 50$) or chemoradiotherapy ($n = 45$). Three patients underwent TRT (twice daily, 45 Gy in total) concurrently with the first course of chemotherapy. Four, 13, and four patients underwent TRT (once daily, 50 Gy in total) concurrently with the second, third, and fourth courses of chemotherapy, respectively. Twenty-one patients underwent TRT (once daily, 50 Gy in total) sequentially after chemotherapy. Among the group A patients, 12 patients underwent TRT concurrently with the third or fourth course of chemotherapy, and seven patients underwent TRT sequentially after chemotherapy. TRT was conducted if the pericardial effusion disappeared after induction chemotherapy. Among the group B patients, 12 patients underwent TRT concurrently with chemotherapy, and 14 patients underwent TRT sequentially (Table 2). Thirteen patients received prophylactic cranial irradiation of 25 Gy (seven patients in group A and six patients in group B).

Figure 2 shows the survival of all 766 patients with SCLC belonging to category M. The survival of patients with LD-M1a was intermediate between those of patients with LD-M0 and ED-M1b ($p < 0.0001$). Six hundred eighty-two patients have died. The median follow-up time was 65.8 months, ranging from 3.2 to 160.1 months. The median survival time among the patients with LD-M1a was 13.4 months (95% CI: 10.7–16.6 months), and the 1-, 2-, 3-, and 5-year survival rates were 56%, 18%, 9%, and 8%, respectively.

Survival analyses for the subgroup of patients with LD-M1a ($n = 96$) are shown in Figures 3, 4 and Table 3. Overall survival was not statistically different between groups A and B ($p = 0.5182$). All 14 patients who received chemotherapy in group A died within 3 years. One patient in group B who received chemotherapy as an initial treatment survived for more than 5 years, but this patient received chemoradiotherapy as a second-line treatment after a local

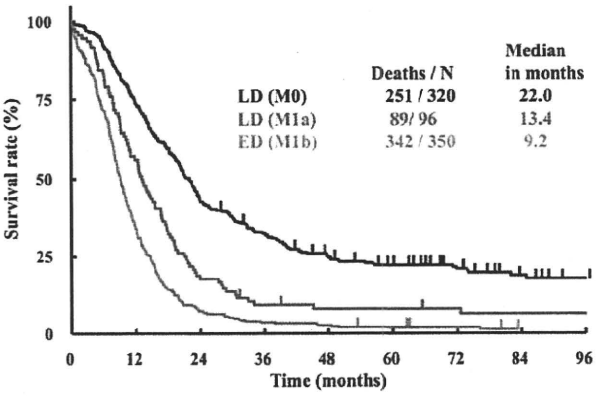

FIGURE 2. Overall survival among all 766 patients with M-category small cell lung cancer. LD, limited disease; ED, extensive disease.

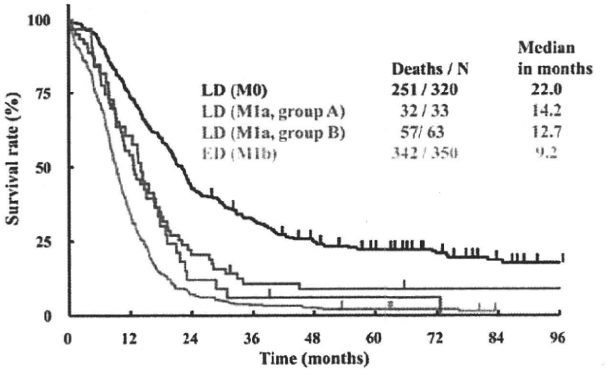

FIGURE 3. Overall survival among patients with M-category small cell lung cancer, subgroups A and B. LD, limited disease; ED, extensive disease.

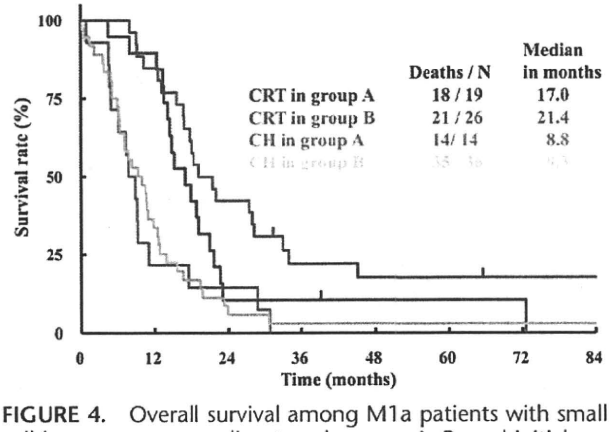

FIGURE 4. Overall survival among M1a patients with small cell lung cancer according to subgroups A, B, and initial treatment delivered. CRT, chemoradiotherapy; CH, chemotherapy.

TABLE 3. Survival Data

Subgroup	No. of Patients	Median Survival Time (mo) (95% CI)	1-yr Survival Rate (%)	2-yr Survival Rate (%)	3-yr Survival Rate (%)	5-yr Survival Rate (%)
ED (M1b)	350	9.2 (8.5–10.0)	34	7	3	2
LD (M0)	320	22.0 (20.0–23.5)	74	43	33	22
LD with pericardial effusion (group A)	33	14.2 (9.1–17.5)	61	12	6	6
Receiving CRT	19	17.0 (13.6–21.0)	89	11	11	11
Receiving Chemotherapy	14	8.8 (4.7–11.1)	21	14	0	0
LD with ipsilateral pleural effusion but without pericardial effusion (group B)	63	12.7 (10.2–16.7)	54	21	11	9
Receiving CRT	26	21.4 (16.7–28.2)	85	42	22	18
Receiving chemotherapy	36	9.3 (6.3–11.8)	33	6	3	3

CI, confidence interval; ED, extensive disease; LD, limited disease; CRT, chemoradiotherapy.

TABLE 4. Six Patients with M1a Small Cell Lung Cancer who Survived for More Than 5 yr

Age (yr)	Sex	Group	Initial Treatment	Survival Time (mo)	State
64	M	A	Chemoradiotherapy	72.6	Dead
70	F	B	Chemoradiotherapy	146.5	Alive
53	M	B	Chemotherapy[a]	140.4	Alive
73	F	B	Chemoradiotherapy	138.0	Alive
72	M	B	Chemoradiotherapy	117.0	Alive
68	M	B	Chemoradiotherapy	65.5	Alive

[a] This patient received chemoradiotherapy as a second-line treatment after a local recurrence. Therefore, all six patients received chemoradiotherapy and achieved long-term survival for more than 5 yr.

M, male; F, female.

recurrence. Four of the 26 patients who received chemoradiotherapy in group B survived for more than 5 years (Table 4). Conversely, only 2 of the 19 patients who received chemoradiotherapy in group A survived for more than 2 years. One patient developed a local recurrence at 4 years and 10 months after the initiation of first-line chemoradiotherapy and died of lung cancer 14 months later. The remaining patient also developed a local recurrence at 2 years and 9 months after the initiation of first-line chemoradiotherapy and received second-line chemotherapy. This patient was still alive at the time of the data cutoff.

DISCUSSION

This retrospective analysis demonstrated that the survival of patients with SCLC and ipsilateral pleural or pericardial effusion (M1a) was intermediate between those of M0 and M1b patients. It is suitable that patients with ipsilateral pleural effusion or pericardial effusion belong to M1a category in the UICC seventh TNM edition. No statistically significant difference in the overall survival between M1a patients with pericardial effusion (group A) and those with ipsilateral pleural effusion but without pericardial effusion (group B) was observed. Among the patients who successfully underwent chemoradiotherapy, the patients in group B had 2-, 3-, and 5-year survival rates of 42%, 22%, and 18%, respectively, whereas the patients in group A had a 2-year survival rate of only 11%. Our previous retrospective analyses demonstrated that the median survival time of patients with cytologically positive and cytologically negative pleural effusion were 9.3 and 12.7 months, respectively. Furthermore, all 11 patients with cytologically positive pleural effusion died within 3 years.[8] Long-term survival for more than 5 years was achieved only by patients with cytologically negative pleural effusion. We speculate that an inflammatory process, such as atelectasis, causes ipsilateral pleural effusion in some patients. Conversely, most pericardial effusion is believed to be malignant. Therefore, long-term survival was seldom achieved by patients with pericardial effusion, even if they received chemoradiotherapy.

Recently, the applicability of the UICC seventh TNM edition for SCLC was investigated using the California Cancer Registry database. This database included 108 and 1518 M1a patients with pericardial effusion and pleural dissemination, respectively. No significant difference in overall survival was observed among patients with pleural or pericardial effusion (median survival time: 7 versus 7 months, 2-year survival rate: 16.7% versus 9.7%, respectively).[10] These data were comparable with our results. Nevertheless, no information regarding the treatment performed for the M1a patients was included in the previous article.

Our retrospective analysis has several limitations. First, the number of M1a patients with pericardial effusion was only 33, because only 8% of the patients with LD-SCLC exhibited pericardial effusion. Second, we did not conduct a cytological examination of the pericardial effusion. Pericardial puncture or drainage is usually performed in patients with cardiac tamponade. None of the patients in group A had cardiac tamponade; therefore, a pericardial puncture was technically difficult. Third, examination period was more than 15 years, from 1992 to 2007. Irinotecan, active for SCLC, has been commonly used from 2000 in Japan. Patients in this study were treated with a potential range of different chemotherapeutic agents during the period, which was not controlled.

Only 2 of 19 patients (11%) who received chemoradiotherapy in group A survived for more than 3 years. Con-

versely, all 14 patients who did not receive chemoradiotherapy in group A died within 3 years. TRT probably improves local control and achieves long-term survival in some patients. Definitive TRT is recommended in M1a patients with SCLC, if ipsilateral pleural or pericardial effusion has disappeared after induction chemotherapy.

In conclusion, the survival of patients with SCLC and ipsilateral pleural or pericardial effusion (M1a) is intermediate between those of M0 and M1b patients. No statistically significant difference in the overall survival of M1a patients with pericardial effusion and those with ipsilateral pleural effusion but without pericardial effusion was observed. Long-term survival was achieved among M1a patients with pericardial effusion who successfully underwent chemoradiotherapy, although 5-year survival rate in these patients was relatively lower than in M1a patients with ipsilateral pleural effusion but without pericardial effusion.

ACKNOWLEDGMENTS

Supported, in part, by a grant from the Ministry of Health, Labor, and Welfare for the third term Comprehensive Strategy for Cancer Control and a Grant-in-Aid for Cancer Research from the Ministry of Health, Labor, and Welfare, Japan.

REFERENCES

1. Zelen M. Keynote address on biostatistics and data retrieval. *Cancer Chemother Rep 3* 1973;4:31–42.
2. Stahel RA, Ginsberg R, Havemann K, et al. Staging and prognostic factors in small cell lung cancer: a consensus report. *Lung Cancer* 1989;5:119–126.
3. Goldstraw P, Crowley J, Chansky K, et al. The IASLC Lung Cancer Staging Project: proposals for the revision of the TNM stage groupings in the forthcoming (seventh) edition of the TNM Classification of malignant tumours. *J Thorac Oncol* 2007;2:706–714.
4. Postmus PE, Brambilla E, Chansky K, et al. The IASLC Lung Cancer Staging Project: proposals for revision of the M descriptors in the forthcoming (seventh) edition of the TNM classification of lung cancer. *J Thorac Oncol* 2007;2:686–693.
5. Rami-Porta R, Ball D, Crowley J, et al. The IASLC Lung Cancer Staging Project: proposals for the revision of the T descriptors in the forthcoming (seventh) edition of the TNM classification for lung cancer. *J Thorac Oncol* 2007;2:593–602.
6. Rusch VW, Crowley J, Giroux DJ, et al. The IASLC Lung Cancer Staging Project: proposals for the revision of the N descriptors in the forthcoming seventh edition of the TNM classification for lung cancer. *J Thorac Oncol* 2007;2:603–612.
7. Shepherd FA, Crowley J, Van Houtte P, et al. The International Association for the Study of Lung Cancer lung cancer staging project: proposals regarding the clinical staging of small cell lung cancer in the forthcoming (seventh) edition of the tumor, node, metastasis classification for lung cancer. *J Thorac Oncol* 2007;2:1067–1077.
8. Niho S, Kubota K, Yoh K, et al. Clinical outcome of chemoradiation therapy in patients with limited-disease small cell lung cancer with ipsilateral pleural effusion. *J Thorac Oncol* 2008;3:723–727.
9. Kaplan EL, Meier P. Nonparametric estimation from incomplete observations. *J Am Stat Assoc* 1958;53:457–481.
10. Ignatius Ou SH, Zell JA. The applicability of the proposed IASLC staging revisions to small cell lung cancer (SCLC) with comparison to the current UICC 6th TNM Edition. *J Thorac Oncol* 2009;4:300–310.

Hepatocellular carcinomas can develop in simple fatty livers in the setting of oxidative stress

Sir,

It is doubtless that non-alcoholic fatty liver disease (NAFLD) has become a critical public health issue in most developed countries.[1] In addition to its close association with metabolic disorders and cardiovascular events, NAFLD itself can progress to life-threatening liver diseases, cirrhosis and hepatocellular carcinoma (HCC).[1,2] Surprisingly, recent clinical observations have revealed that HCC can develop in non-cirrhotic, but steatotic livers without significant fibrosis.[3,4] In the reports, authors emphasised the importance of underlying metabolic disorders and oxidative stress in hepatocarcinogenesis in such NAFLD cases.

We herein report a case of NAFLD complicated by HCC, in which the potential contribution of oxidative stress to hepatocarcinogenesis in NAFLD has been further strongly suggested.

In May 2006, a 72-year-old obese Japanese man was admitted to the National Hospital Organization Osaka National Hospital, Japan, because of a hepatic nodule. The patient had a 5 year medical history of hypertension and fatty liver. He underwent an operation for abdominal aortic aneurysm in April 2004, and had since been an outpatient. Follow-up abdominal ultrasonography showed, in addition to hepatic steatosis, a nodular lesion approximately 2 cm in diameter in the left lobe of the liver. The hepatic nodule had been growing larger, and findings of computed tomography (CT) strongly suggested that it was HCC (Fig. 1).

On admission, he appeared to be healthy except for obesity, and the laboratory test results showed normal serum levels of transaminases and negativity for hepatitis B and C viruses. After the examinations, under the tentative diagnosis of HCC, a surgical operation was performed to remove the left lobe of the liver. The cut surface of the liver sample was smooth and yellowish-brown, and demonstrated the clearly circumscribed nodule 5 cm in diameter (Fig. 2). Histological examination revealed that the nodular lesion was well-differentiated HCC (Fig. 3A), and the background hepatic disorder was simple steatosis without inflammation and fibrosis (Fig. 3B). Routine pathological examination couldn't detect any causative factors in hepatocarcinogenesis, such as iron overload. However, an immunohistochemical analysis revealed that as well as tumour cells, a few non-tumourous hepatocytes showed immunoreactivity for anti-oxidised phosphatidylcholine (oxPC; Fig. 3A,B insets), a marker of

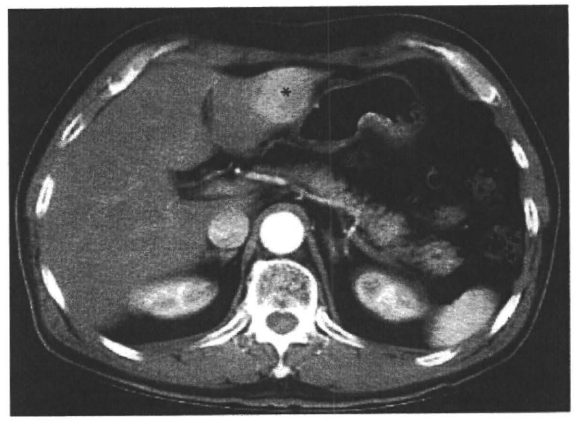

Fig. 1 Findings of computed tomography. A hypervascular nodule is seen in the left lobe of the liver (asterisk).

Fig. 2 The cut-surface of the liver sample. A well-circumscribed nodular lesion 5 cm in diameter is present.

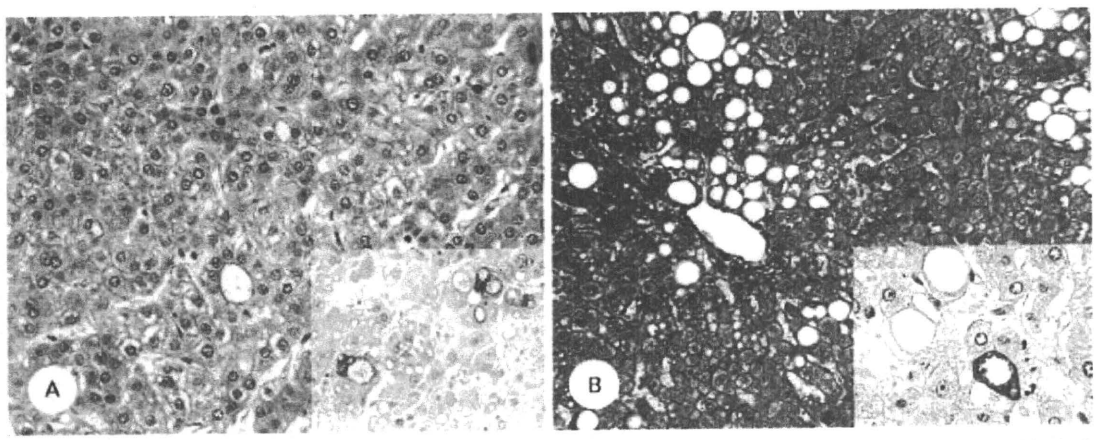

Fig. 3 Microscopic findings of the liver sample. (A) The hepatic nodule consists of well-differentiated HCC (H&E). (B) A background liver condition is simple steatosis without fibrosis (Azan-Mallory stain for collagen). Insets: steatotic liver cells of both tumourous and non-tumourous portions are positive for oxPC (immunoperoxidase with anti-oxPC).

oxidative cellular injury.[5] The immunoreactivity was found restrictively in steatotic cells in both tumourous and non-tumourous portions. It suggested that the steatosis-related oxidative hepatocellular injury had persisted and had played a certain role in the development of HCC. His postoperative course was uneventful and he was discharged. Follow-up examinations have been done every 3 months, resulting in no evidence of tumour recurrence. When last seen, in December 2009, he was well.

Like the present case, HCC can develop in non-inflammatory, non-fibrotic, but steatotic livers. A previous case report of HCC arising in the absence of advanced NAFLD emphasised the potential roles for metabolic factors (diabetes, hypertension, obesity and dyslipidaemia) and oxidative stress in hepatocarcinogenesis.[4] Oxidative stress is generally recognised as an important factor in hepatocarcinogenesis.[2,6] Our immunohistochemical results showed oxPC-positive steatotic hepatocytes in the background liver tissue of HCC. OxPC, one of the lipid peroxides, is a highly specific marker of oxidative damage. In our previous observation, its immunoreactivity was seen mainly in steatotic or degenerated hepatocytes in NAFLD, and only in some Kupffer cells in normal liver tissues.[5] Hence, the present result suggested that the fatty liver had chronically been exposed to oxidative stress, which was probably initiated prior to hepatocarcinogenesis. To our knowledge, this is the first direct evidence of oxidative hepatocellular injury occurring in simple fatty livers complicated by HCC. Excess fat accumulation itself, even in the absence of inflammation, can be a source of oxidative stress that induces hepatocarcinogenesis. In conclusion, simple steatosis-related oxidative stress should be considered as one of the risk factors of HCC.

Yoshihiro Ikura*
Eiji Mita†
Shoji Nakamori‡

**Department of Pathology, Osaka City University Graduate School of Medicine, Osaka, †Departments of Gastroenterology, and ‡Surgery, National Hospital Organization, Osaka National Hospital, Osaka, Japan*

Contact Dr Y. Ikura.
E-mail: ikura@med.osaka-cu.ac.jp

1. Neuschwander-Tetri BA, Caldwell SH. Nonalcoholic steatohepatitis: summary of an AASLD Single Topic Conference. *Hepatology* 2003; 37: 1202–19.
2. Caldwell SH, Crespo DM, Kang HS, Al-Osaimi AM. Obesity and hepatocellular carcinoma. *Gastroenterology* 2004; 127(Suppl 1): S97–103.
3. Paradis V, Zalinski S, Chelbi E, Guedj N, Degos F, Vilgrain V, *et al.* Hepatocellular carcinomas in patients with metabolic syndrome often develop without significant liver fibrosis: a pathological analysis. *Hepatology* 2009; 49: 851–9.
4. Guzman G, Brunt EM, Petrovic LM, Chejfec G, Layden TJ, Cotler SJ. Does nonalcoholic fatty liver disease predispose patients to hepatocellular carcinoma in the absence of cirrhosis? *Arch Pathol Lab Med* 2008; 132: 1761–6.
5. Ikura Y, Ohsawa M, Suekane T, *et al.* Localization of oxidized phosphatidylcholine in nonalcoholic fatty liver disease: impact on disease progression. *Hepatology* 2006; 43: 506–14.
6. Sasaki Y. Does oxidative stress participate in the development of hepatocellular carcinoma? *J Gastroenterol* 2006; 41: 1135–48.

DOI: 10.1097/PAT.0b013e32834274ec

Benign prostatic glands as a tissue component of testicular teratoma: an uncommon histological finding

Sir,

The occurrence of benign prostatic tissue as a component of testicular teratoma has only been described as a single case report.[1] This may be due to its rare occurrence, as well as the failure of the diagnostic pathologist to recognise glands as prostatic on routine sections and to subsequently confirm this by immunohistochemistry. In our laboratory we utilise Solufix (Tissugen, Australia), a glutaraldehyde-based tissue fixative for routine histology. This agent preserves the spermine content of prostatic secretory granules (PSG) which stain intensely with eosin on routine stains allowing easy recognition of prostatic epithelium.[2]

We present two cases of benign prostatic glandular tissue occurring in two patients with primary testicular tumours; a mature teratoma in a 35-year-old male and a mixed germ cell tumour (30% mature teratoma) in a 39-year-old male. Each patient underwent routine inguinal orchidectomy for a clinically detected testicular mass.

On microscopy, benign gland structures were recognised which were lined by two cell types and bore some resemblance to prostatic acini. These glands were highlighted by their intense eosinophilic PSG (Fig. 1 and 2), and were distributed either singularly or as clusters separated by bland stroma. Lining epithelium showed variable morphology ranging from bland epithelial cells consistent with benign prostatic glands (Fig. 1) to epithelial cells with larger nuclei and prominent nucleoli (Fig. 2), consistent with prostatic intraepithelial neoplasia (PIN). The prostatic nature of the glands was subsequently confirmed by strong diffuse cytoplasmic reactivity with immunohistochemistry for PSA (Dako, USA; Fig. 1 inset) and prostatic acid phosphatase (Dako; not shown). Basal cells were confirmed with immunostaining for high molecular weight cytokeratin 34βE12 (Dako; Fig. 2 inset).

Recognition of the first case prompted a histological review of all testicular teratomas over a 10 year period which included 20 testicular tumours comprising pure teratomas ($n = 10$) and mixed germ cell tumours with a mature teratoma component of $>10\%$ ($n = 10$). This review identified the second case,

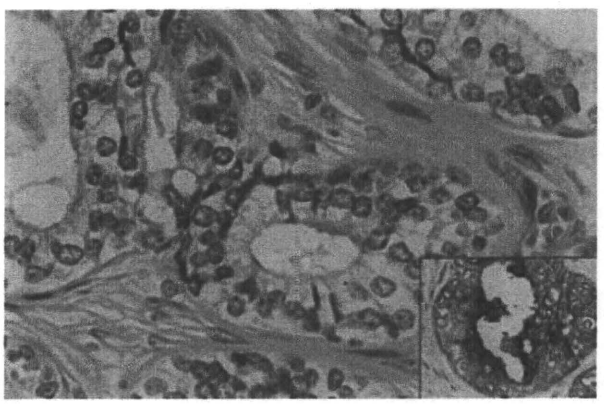

Fig. 1 Benign prostatic glands within a testicular germ cell tumour surrounded by bland stroma. Small eosinophilic granules (prostate secretory granules) are seen in the apical cytoplasm confirming prostatic epithelial differentiation. Inset: These cells are strongly labelled with PSA immunostaining.

Glycobiology vol. 21 no. 2 pp. 235–246, 2011
doi:10.1093/glycob/cwq154
Advance Access publication on October 25, 2010

Expression and the role of 3′-phosphoadenosine 5′-phosphosulfate transporters in human colorectal carcinoma

Shin Kamiyama[2,3,11*], Tomomi Ichimiya[2,*], Yuzuru Ikehara[4], Tomofumi Takase[2], Izumi Fujimoto[2], Takeshi Suda[2], Shoji Nakamori[5], Mitsuru Nakamura[6], Fumiaki Nakayama[7], Tatsuro Irimura[8], Hayao Nakanishi[9], Masahiko Watanabe[10,12], Hisashi Narimatsu[4], and Shoko Nishihara[1,2]

[2]Laboratory of Cell Biology, Department of Bioinformatics, Soka University, 1–236 Tangi-cho, Hachioji, Tokyo 192-8577; [3]Research Association for Biotechnology, 3-9, Nishi-Shinbashi 2-chome, Minato-ku, Tokyo 105-0003; [4]Research Center for Medical Glycoscience (RCMG), National Institute of Advanced Industrial Science and Technology (AIST), 1-1-1 Umezono, Tsukuba, Ibaraki 305-8568; [5]Department of Surgery, Osaka National Hospital, National Hospital Organization, 2-1-14 Houenzaka, Chuo-ku, Osaka 540-0006; [6]East Hospital, Kitasato University, 2-1-1 Asamizodai, Sagamihara, Kanagawa 228-8520; [7]Department of Radiation Emergency Medicine, National Institute of Radiological Sciences, 4-9-1 Anagawa, Inage-ku, Chiba 263-8555; [8]Laboratory of Cancer Biology and Molecular Immunology, Graduate School of Pharmaceutical Sciences, The University of Tokyo, 7-3-1 Hongo, Bunkyo-ku, Tokyo 113-0033; [9]Division of Oncological Pathology, Aichi Cancer Center Research Institute, 1-1 Kanokoden, Chikusa-ku, Nagoya, Aichi 464-8681; and [10]Department of Surgery, School of Medicine, Keio University, 35 Shinanomachi, Shinjuku-ku, 160-8582 Tokyo, Japan

Received on January 31, 2010; revised on September 7, 2010; accepted on September 23, 2010

Sulfation represents an essential modification for various molecules and regulates many biological processes. The sulfation of glycans requires a specific transporter for 3′-phosphoadenosine 5′-phosphosulfate (PAPS) on the Golgi apparatus. This study investigated the expression of PAPS transporter genes in colorectal carcinomas and the significance of Golgi-specific sulfation in the proliferation of colorectal carcinoma cells. The relative amount of *PAPST1* transcripts was found to be higher than those of *PAPST2* in colorectal cancerous tissues. Immunohistochemically, the enhanced expression of PAPST1 was observed in fibroblasts in the vicinity of invasive cancer cells, whereas the expression of PAPST2 was decreased in the epithelial cells. RNA interference of either of the two PAPS transporter genes reduced the extent of sulfation of cellular proteins and cellular proliferation of DLD-1 human colorectal carcinoma cells. Silencing the PAPS transporter genes reduced fibroblast growth factor signaling in DLD-1 cells. These findings indicate that PAPS transporters play a role in the proliferation of colorectal carcinoma cells themselves and take part in a desmoplastic reaction to support cancer growth by controlling their sulfation status.

Keywords: colorectal carcinoma/heparan sulfate/PAPST1/PAPS transporter/sulfation

Introduction

In malignant transformation, specific carbohydrate antigens are expressed on glycoproteins or glycolipids on the surface of cancer cells. Appearance of these carbohydrate epitopes is associated with alterations in the expression of several glycosyltransferases. These carbohydrate epitopes play important roles in the progression and metastasis of cancer cells and are used as typical tumor markers for the diagnosis of various human cancers. In addition, it has been reported that certain nucleotide sugar transporters are involved in the expression of carbohydrate epitopes in cancer. Nucleotide sugar transporters are proteins that are localized on membranes of the endoplasmic reticulum or the Golgi apparatus. These proteins provide substrates for glycosyltransferases in the lumen. Kumamoto et al. (2001) reported that the expression of uridine diphosphate (UDP)-galactose transporter (solute carrier family 35, member A2; SCL35A2) is increased in human colon carcinoma and is responsible for the synthesis of the Thomsen–Friedenreich antigen and sialyl Lewis A (Le^a) and X (Le^x) epitopes. Moriwaki et al. (2007) reported that guanidine diphosphate (GDP)-fucose transporter (SLC35C1) expression is upregulated in hepatocellular carcinoma and plays a role in an increased rate of fucosylation. These reports suggest that the expression of nucleotide sugar transporters is a key factor for regulating the synthesis of carbohydrate epitopes in cancer cells.

Another essential modification is sulfation which is frequently found on the glycans of proteoglycans, glycolipids, and glycoproteins, and on tyrosine residues of proteins. Sulfation is catalyzed by various sulfotransferases, and it modifies the properties of molecules by imparting a negative charge. Heparan sulfate (HS) and chondroitin sulfate (CS) proteoglycans are well-characterized macromolecules that have highly sulfated glycosaminoglycan (GAG) chains and play significant roles in many biological processes. Inhibition of

*The first two authors contributed equally to this article.

[11]Present address: Department of Health and Nutrition, Faculty of Human Life Studies, University of Niigata Prefecture, 471 Ebigase, Higashi-ku, Niigata 950-8680, Japan
[12]Present address: Department of Surgery, School of Medicine, Kitasato University, 1-15-1 Kitasato Sagamihara, Kanagawa 228-8555, Japan
[1]To whom correspondence should be addressed: Tel: +81-42-691-8140; Fax: +81-42-691-8140; e-mail: shoko@soka.ac.jp

sulfation using chlorate, an inhibitor of 3′-phosphoadenosine 5′-phosphosulfate (PAPS) sulfurylase, reduces the signaling of various growth factors such as the fibroblast growth factor (FGF) (Rapraeger et al. 1991; Yayon et al. 1991) and Wnt (Reichsman et al. 1996). Analysis of *Drosophila* mutants with defects in sulfotransferases revealed the importance of sulfation of GAGs on growth factor signaling during development (Lin and Perrimon 1999; Lin et al. 1999; Kamimura et al. 2001, 2006).

On the other hand, it has been reported that some sulfated structures alter the expression of molecules associated with the progression of cancer. Sulfated sialyl Le^x epitopes have been identified as ligands for L-selectin (Mitsuoka et al. 1998), which plays a crucial role in the leukocyte homing process in high endothelial venules. It is known that the risk of malignancy in colorectal cancer is associated with an increase in sialylation (Nakamori et al. 1993; Matsushita et al. 1995; Nakayama et al. 1995) and a decrease in sulfation of carbohydrate epitopes (Yamori et al. 1989; Irimura et al. 1991; Matsushita et al. 1995; Izawa et al. 2000). Immunohistochemical studies have revealed that the goblet cells of human colonic epithelia of Lewis-positive individuals show a strong signal for sulfated mucins (Tsuiji et al. 1998b). The expression of sulfomucins is much lower in colon adenocarcinomas than in the normal mucosa due to the decreased expression of specific sulfotransferases (Seko et al. 2002b).

Two PAPS transporter genes have been previously identified in both humans and *Drosophila* (Kamiyama et al. 2003, 2006; Goda et al. 2006). Lüders et al. (2003) independently reported that *slalom* is a PAPS transporter gene in *Drosophila*. These PAPS transporters are required for the sulfation of cellular proteins and normal development in *Drosophila* (Kamiyama et al. 2003; Lüders et al. 2003; Goda et al. 2006). Additionally, both human PAPST1 (SLC35B2) and PAPST2 (SLC35B3) were found to be involved in the sulfation of the 6-sulfolactosamine epitope in a human colorectal carcinoma cell line (Kamiyama et al. 2006). Huopaniemi et al. (2004) reported that the CMP-sialic acid transporter (SLC35A1), the GDP-fucose transporter (SLC35C1) and the PAPS transporter (SLC35B2) are involved in coordinated transcriptional regulation during induction of sialyl sulfo-Le^x glycan biosynthesis during acute inflammation. These studies indicate that PAPS transporters regulate the sulfation process in addition to sulfotransferases; however, studies have not been conducted on the expression status of PAPS transporter genes in cancer. Therefore, in the present study, we investigated the expression of PAPS transporter genes in colorectal carcinomas and their role in the regulation of sulfation in colorectal carcinoma cells. The significance of Golgi-specific sulfation in proliferation of colorectal carcinoma cells is also discussed.

Results

Expression status of PAPS transporter genes in colorectal carcinomas

Previously, we identified two human PAPS transporter genes: *PAPST1* and *PAPST2* (Kamiyama et al. 2003, 2006). In normal colon tissue, *PAPST1* was expressed at substantially lower level than *PAPST2* (Kamiyama et al. 2006). In the present study, the expression of these PAPS transporter genes in human colorectal carcinomas was investigated. Initially, the expression levels of these transcripts in colorectal carcinoma cell lines were quantified using real-time polymerase chain reaction (PCR). The relative expression level of *PAPST1* transcripts was higher than that of *PAPST2* in all of the 22 colorectal carcinoma cell lines tested (Figure 1A).

Subsequently, the expression levels of *PAPST1* and *PAPST2* were determined in human colorectal tissues. Figure 1B indicates the expression levels of *PAPST1* and *PAPST2* transcripts in cancerous and noncancerous colorectal tissues obtained from seven specimens. Consistent with the result from the cell lines, the relative amount of *PAPST1* transcripts was higher than that of *PAPST2* in colorectal cancerous tissues. Meanwhile, a considerable amount of *PAPST1* transcripts was detected in noncancerous colorectal tissues. In the previous study, we used only one sample for the determination of *PAPST1* and *PAPST2* expression in human colon tissue (Kamiyama et al. 2006). Therefore, the difference might be due to the individual and/or position-specific differences. The expression of *PAPST2* was found to be decreased in colorectal cancerous tissues.

The expression of *PAPST1* mRNA in colorectal carcinoma was confirmed through *in situ* hybridization. As shown in Figure 2A, *PAPST1* mRNA was detected in both adenocarcinoma cells and the stromal cells. To further characterize the distribution of PAPST1 in colorectal tissues, we prepared an antibody against a C-terminal peptide of mouse PAPST1. The immunoreactivity of the anti-PAPST1 antibody to human PAPST1 protein was confirmed by western blot analysis against c-myc-tagged human PAPST1 protein, which was expressed in HEK293 cells (Figure 2C). The anti-PAPST1 antibody specifically recognized both endogenous (Figure 2D, left and middle lanes) and c-myc-tagged human PAPST1 protein (Figure 2D, right lane). Immunohistochemical analysis identified that the predominant expression of PAPST1 is on epithelial cells rather than on stromal cells in both noncancerous (Figure 2E and E′) and cancerous (Figure 2F and F′) colorectal tissues. The expression levels of PAPST1 protein in epithelial cells were similar in cancerous and noncancerous tissues, whereas the observed levels of stromal cells were region-specific and dispersed (Figure 2G, G′ and I, arrows). Moreover, enhanced expression of PAPST1 was also observed in fibroblasts in the vicinity of invasive cancer cells (Figure 2I, asterisks). This suggests that the desmoplastic reaction is associated with elevated levels of PAPST1 in cancerous tissue. PAPST1 protein was detected in all cancerous and noncancerous sections tested in the perinuclear region (Golgi apparatus) of the cells (Figure 2G, G′ and H, arrowheads).

On the other hand, PAPST2 protein was predominantly detected in epithelial cells in noncancerous colorectal tissues (Figure 2J). However, the expression of PAPST2 protein in epithelial cells was faintly detectable in cancerous colorectal tissues (Figure 2K). Strong expression of PAPST2 protein was observed in cells of hematopoietic lineage in both noncancerous and cancerous tissues (Figure 2J and K, diamond arrows). These results indicate that colorectal cancerous tissue increases the expression of PAPST1 in fibroblasts in the vicinity of the desmoplastic reaction and decreases the expression of PAPST2 in epithelial carcinoma cells.

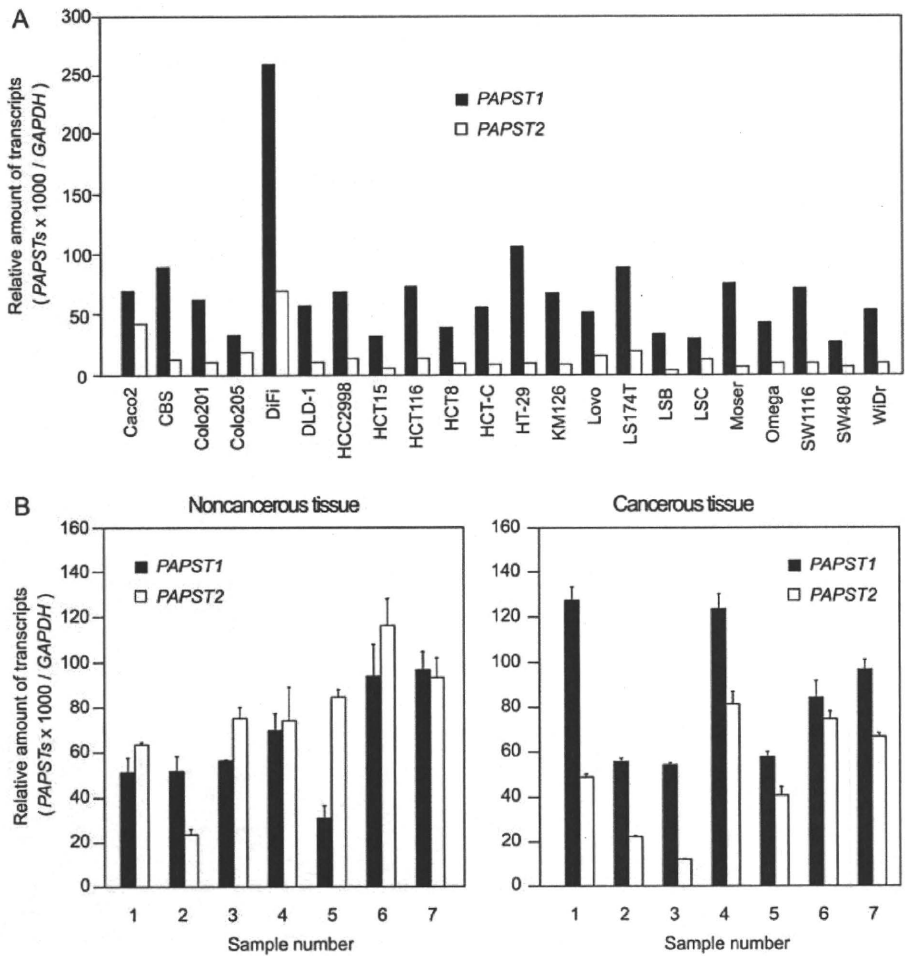

Fig. 1. Quantitative analysis of *PAPST1* and *PAPST2* transcripts in colorectal carcinoma cell lines (**A**) and noncancerous and cancerous human colorectal tissues (**B**). The amounts of *PAPST1* and *PAPST2* transcripts were determined using real-time PCR. The obtained values were normalized with respect to the amount of *GAPDH* transcripts in the same cDNA. Sample information is described in Table I. Left panel, noncancerous tissue, right panel, cancerous tissue.

Table I. Histopathological characteristics of colorectal carcinomas

Sample no.	Site of carcinoma	Histopathological diagnosis
1	Cecum	Moderately differentiated adenocarcinoma
2	Right hemi-colon	Well-differentiated adenocarcinoma
3	Ascending colon	Mucinous adenocarcinoma
4	Sigmoid colon	Moderately differentiated adenocarcinoma
5	Sigmoid colon	Moderately differentiated adenocarcinoma
6	Sigmoid colon	Well-differentiated adenocarcinoma
7	Sigmoid colon	Well-differentiated adenocarcinoma

Sulfated glycoconjugates in colorectal carcinoma cell lines

The sulfation status of cellular proteins in colorectal carcinoma cell lines was investigated using three cell lines, Omega, DLD-1 and LS174T, which were reported as possessing sulfated glycoconjugates (Tsuiji et al. 1998a). These cell lines were metabolically labeled with $Na_2[^{35}S]O_4$ for 24 h and the incorporation of radioactivity into cellular proteins was analyzed (Figure 3A). In all three cell lines, a broad band above 200 kDa was observed (Figure 3A, arrowhead). This signal mostly disappeared when cells were treated with heparitinase, indicating the presence of HS. Omega cells, but not the other two cell lines, exhibited a band at a higher molecular range (Figure 3A, arrow). This signal was derived from CS, as it disappeared upon treatment with chondroitinase ABC. LS174T retained a dense band even after treatment with heparitinase and chondroitinase ABC. Because LS174T is known to have high levels of sulfated mucins (Tsuiji et al. 1998a), this signal was attributed to the sulfated mucins.

The ratio of sulfate incorporation into HS, CS and *N*-glycans was determined in these cell lines. The levels of sulfate incorporation into HS, CS and *N*-glycans were estimated on the basis of the radioactivity released by the treatment of cells or cellular proteins with heparitinase, chondroitinase ABC and PNGase F (peptide:*N*-glycosidase F), respectively. The level of total sulfate incorporation into the proteins was determined from the radioactivity of proteins precipitated with trichloroacetic acid (TCA). Figure 3B shows the ratio of sulfate incorporation into HS, CS, *N*-glycans and

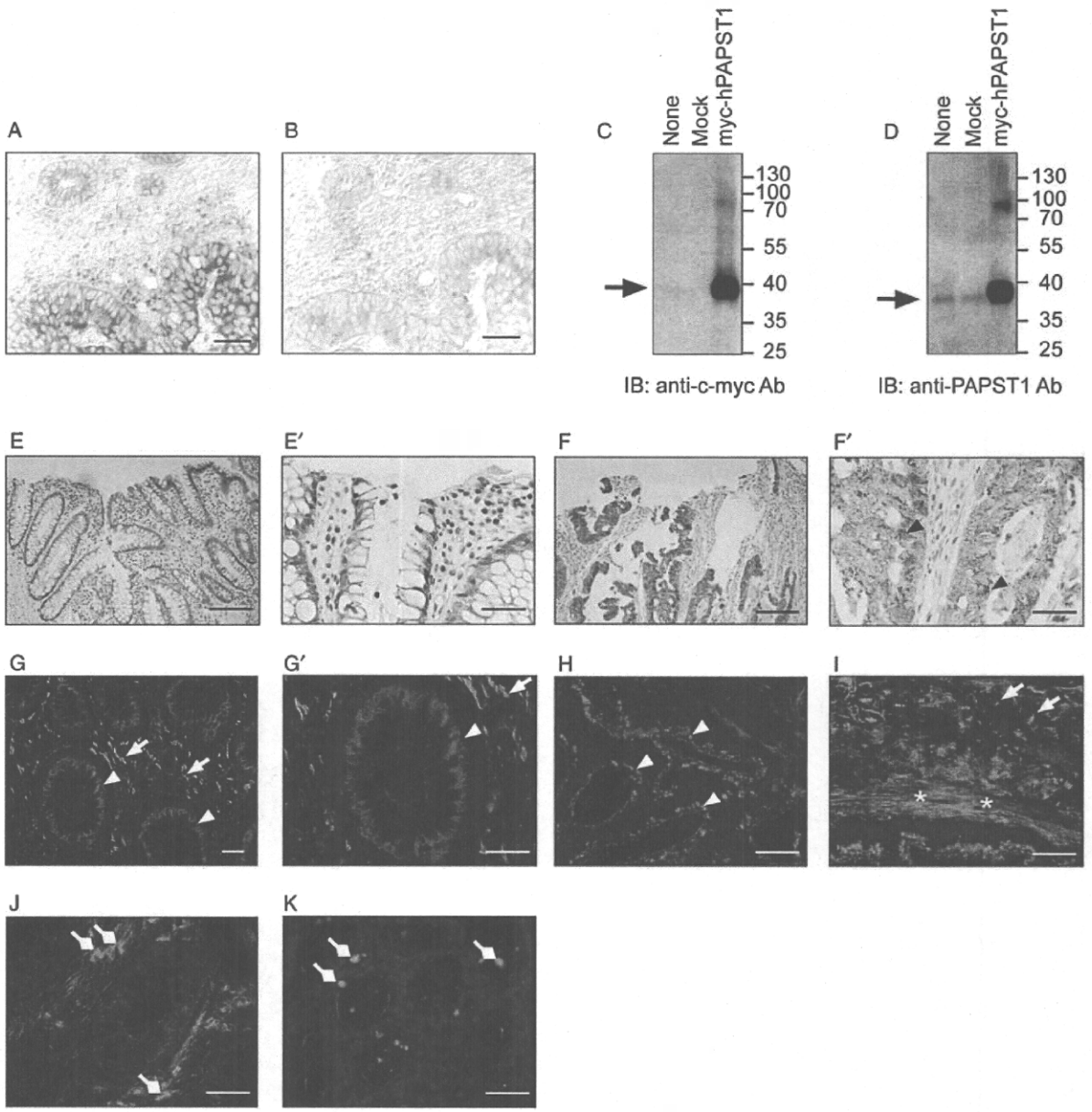

Fig. 2. In situ hybridization of *PAPST1* mRNA and immunohistochemical staining for PAPST1 and PAPST2 proteins in colorectal carcinoma. (**A** and **B**) Serial frozen sections from rectal carcinoma were hybridized with either a digoxigenin-labeled antisense (A) or sense (B) riboprobe against *PAPST1* mRNA. Hybridized probes were detected with an alkaline phosphatase-labeled anti-digoxigenin antibody. Bar scales are 50 μm. (**C** and **D**) The specificity of anti-PAPST1 antibody to human PAPST1 (hPAPST1) protein. A pCXN2-c-myc expression vector containing the *hPAPST1* gene was transfected into HEK293 cells and the cell lysate was prepared. hPAPST1 protein was detected by western blotting using anti-c-myc (C) or anti-PAPST1 (D) antibodies. Arrows indicate the band of hPAPST1 protein. None, intact cells; mock, cells treated with empty vector; myc-hPAPST1, cells treated with pCXN2-c-myc-hPAPST1. IB, immunoblot; Ab, antibody. (**E**–**F′**) Paraffin-embedded sections were immunostained with anti-PAPST1 antibody using an automated Ventana system. Sections were counterstained with hematoxylin. (E and E′) Noncancerous colorectal tissue and (F and F′) cancerous colorectal tissue. PAPST1 protein was predominantly detected as perinuclear dots in epithelial carcinoma cells (F′, arrowheads). In both noncancerous (E and E′) and cancerous (F and F′) colorectal tissues, stromal cells were weakly stained, whereas epithelial cells were strongly stained. Representative results from 19 (E) and 20 (F) stains are shown. Bar scales are 200 μm (E and F) and 50 μm (E′ and F′). (E and F), low magnification; (E′ and F′), high magnification. (**G**–**K**) Frozen sections were immunostained with anti-PAPST1 (G–I) or anti-PAPST2 (J and K) antibody and detected with anti-rabbit IgG conjugated Alexa Flour 488 (green). F-actin filaments and nuclei were counterstained with phallotoxin-conjugated Alexa Fluor 594 (red) and with Hoechst 33342 (blue), respectively. (G, G′ and J) Noncancerous colorectal tissues and (H, I and K) cancerous colorectal tissues. In both noncancerous and cancerous colorectal tissues, PAPST1 protein was detected in the perinuclear region (Golgi apparatus) of epithelial cells (G, G′ and H, arrowheads) and stromal cells (G, G′ and I, arrows). Fibroblasts were heavily stained with PAPST1 antibody in the vicinity of invasive cancer cells where the desmoplastic reaction was observed (I, asterisks). PAPST2 protein was strongly detected in cells of hematopoietic lineage (diamond arrows) in both noncancerous (J) and cancerous (K) colorectal tissues. Epithelial cells were stained with anti-PAPST2 antibody in noncancerous colorectal tissues (J), whereas they were only faintly stained in cancerous colorectal tissues (K). Bar scales are 50 μm. (G), low magnification; (G′), high magnification.

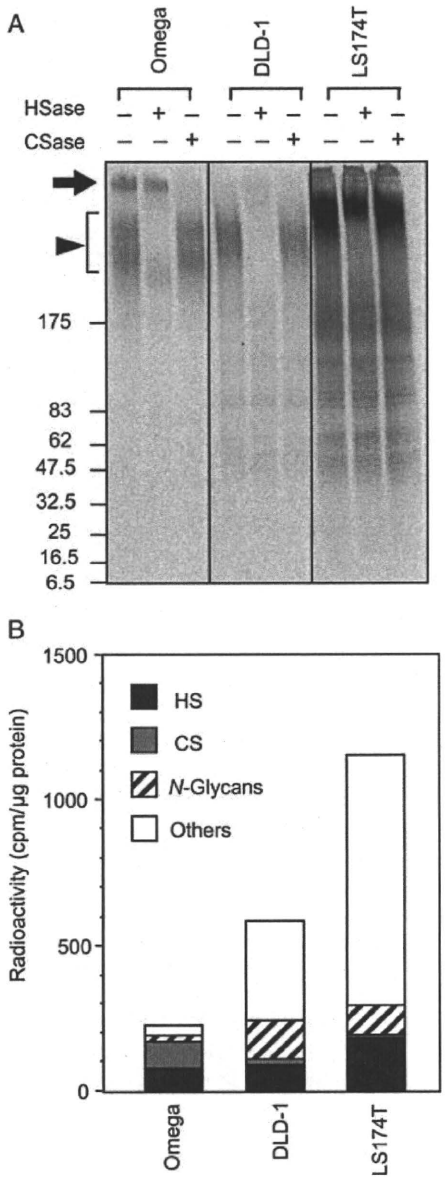

Fig. 3. Metabolic labeling of colorectal carcinoma cell lines. (**A**) Autoradiograph of radioactivity incorporated into cellular proteins. Omega, DLD-1 and LS174T cells were labeled with $Na_2[^{35}S]O_4$ for 24 h and treated in the presence or absence of heparitinase (HSase) or chondroitinase ABC (CSase) for 2 h. Cellular proteins were separated by 2–15% gradient SDS–PAGE. The arrowhead and arrow indicate signals that disappear upon treatment with HSase and CSase, respectively. (**B**) The ratio of sulfate incorporation into HS, CS and *N*-glycans in cellular proteins. The amounts of sulfate incorporated into HS, CS and *N*-glycans were estimated on the basis of the radioactivity released after treatment of cells or cellular proteins with HSase, CSase and PNGase F, respectively. The amount of total sulfate incorporation into proteins was determined by precipitation of the proteins in the cell lysate with TCA.

other glycans. Consistent with the results of autoradiography, Omega cells were found to contain high levels of HS and CS and lower levels of sulfated *N*-glycans. DLD-1 and LS174T cells had low levels of CS but high levels of HS and

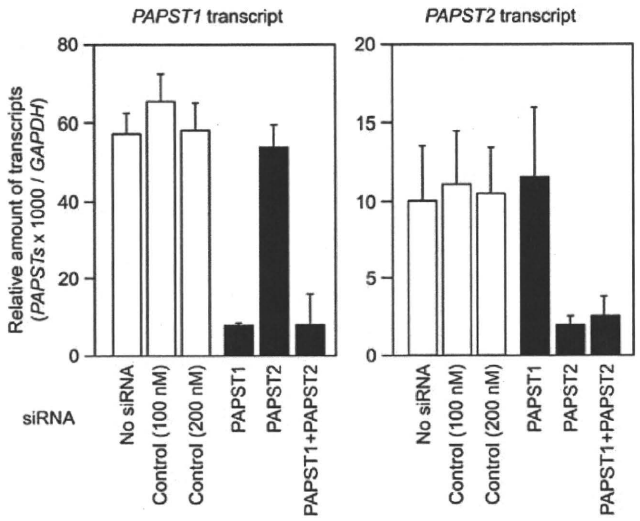

Fig. 4. Knockdown efficiency of each siRNA for *PAPST1* (left panel) and *PAPST2* (right panel) transcripts. Relative amounts of each transcript were quantified using real-time PCR and normalized with respect to the amount of *GAPDH*. Values shown are means (SDs) obtained from three independent experiments. No siRNA, cells treated with no siRNA; control (100 nM), cells treated with 100 nM control siRNA; control (200 nM), cells treated with 200 nM control siRNA; PAPST1, cells treated with 100 nM *PAPST1* siRNA; PAPST2, cells treated with 100 nM *PAPST2* siRNA; PAPST1 + PAPST2, cells treated with 100 nM *PAPST1* siRNA and 100 nM *PAPST2* siRNA.

N-glycans. LS174T contained a substantial amount of extra sulfate, which was considered to be represented by sulfated mucins and sulfated tyrosine residues of proteins.

Gene silencing of PAPS transporters reduces sulfation in DLD-1 cells

To address whether the expression status of PAPS transporters affects sulfation in colorectal carcinomas, the expression of PAPS transporter genes in a colorectal carcinoma cell line was reduced via RNA interference (RNAi). For the RNAi experiments, *PAPST1* siRNA (small interfering RNA), *PAPST2* siRNA and a control siRNA that did not match any human gene were used. On the basis of knockdown efficiency, DLD-1 was selected among the three cell lines. We decided to introduce siRNA in three separate sequential additions because a single addition was found to have a slight effect on the sulfation modification. On days 1, 4 and 7, each of these siRNAs was repeatedly transfected into DLD-1 cells, and the knockdown efficiency was determined by real-time PCR on day 10 (i.e. 3 days after the third transfection). Figure 4 shows the expression of *PAPST1* and *PAPST2* genes in DLD-1 cells treated with each siRNA. Treatment with *PAPST1* and *PAPST2* siRNAs was found to reduce the expression level of the corresponding gene to <20% of the original level. Double knockdown with *PAPST1* and *PAPST2* siRNAs reduced both transcripts in the DLD-1 cells. No significant alteration was observed in the expression level of the nontargeted gene.

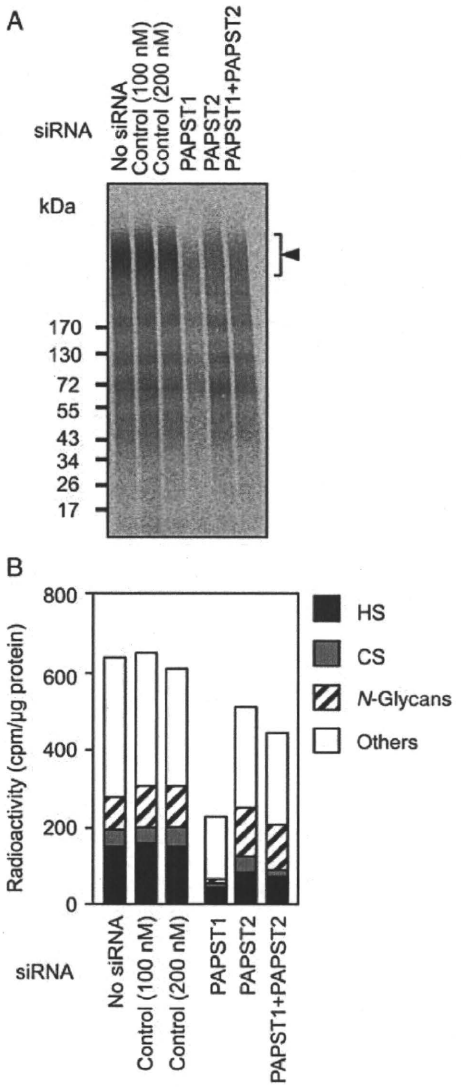

Fig. 5. Metabolic labeling of DLD-1 cells treated with siRNAs. DLD-1 cells were treated with various siRNAs on days 1, 4 and 7 and analyzed on day 10. (**A**) Autoradiograph of incorporated radioactivity into cellular proteins. Cells treated with each siRNA were labeled with $Na_2[^{35}S]O_4$ for 24 h and analyzed as described in Experimental procedures. Cellular proteins were separated by 2–15% gradient SDS–PAGE. The arrowhead indicates the signal that disappeared upon treatment with HSase. (**B**) Ratio of sulfate incorporation into HS, CS and *N*-glycans in cellular proteins. The amounts of incorporated sulfate into HS, CS and *N*-glycans were estimated on the basis of the radioactivity released after the treatment of cells or cellular proteins with HSase, CSase and PNGase F, respectively. The amount of total sulfate incorporation into proteins was determined by the precipitation of the proteins in the cell lysate with TCA. No siRNA, cells treated with no siRNA; control (100 nM), cells treated with 100 nM control siRNA; control (200 nM), cells treated with 200 nM control siRNA; PAPST1, cells treated with 100 nM *PAPST1* siRNA; PAPST2, cells treated with 100 nM *PAPST2* siRNA; PAPST1+PAPST2, cells treated with 100 nM *PAPST1* siRNA and 100 nM *PAPST2* siRNA.

On day 9 (i.e. 2 days after the third transfection), the cells were labeled with $Na_2[^{35}S]O_4$ for 24 h. Figure 5A shows the autoradiograph of the cellular proteins in the cell lysates.

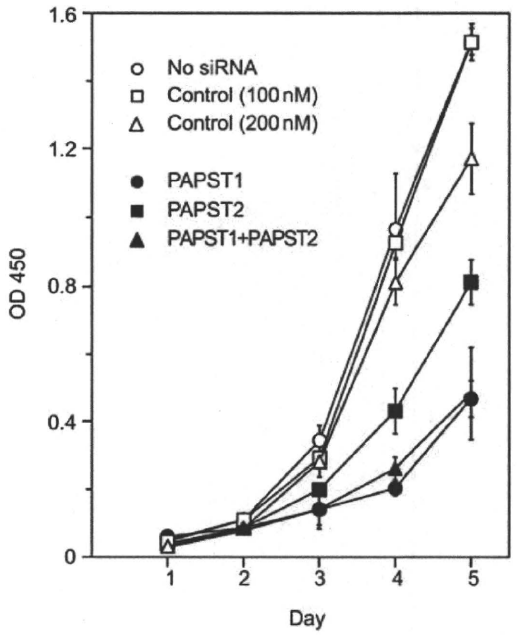

Fig. 6. Cellular proliferation of DLD-1 cells treated with siRNA. DLD-1 cells were transfected with each siRNA on days 1, 4 and 7 and seeded onto a 96-well plate on day 8. The number of cells was quantified once per day for 5 days using the WST-8 assay. No siRNA, cells treated with no siRNA; control (100 nM), cells treated with 100 nM control siRNA; control (200 nM), cells treated with 200 nM control siRNA; PAPST1, cells treated with 100 nM *PAPST1* siRNA; PAPST2, cells treated with 100 nM *PAPST2* siRNA; PAPST1+PAPST2, cells treated with 100 nM *PAPST1* siRNA and 100 nM *PAPST2* siRNA.

Treatment with either *PAPST1* or *PAPST2* siRNA reduced the density of HS (Figure 5A, arrowhead) and other signals. Figure 5B shows the sulfate incorporation into HS, CS, *N*-glycans and other glycans in the DLD-1 cells treated with each siRNA. The cells treated with *PAPST1* siRNA reduced the extent of sulfate incorporation into HS to one-third that of the cells treated with control siRNA. Treatment with *PAPST2* siRNA was less effective; the extent of sulfate incorporation into HS was half that of the cells treated with control siRNA. In the DLD-1 cells, treatment with *PAPST1* siRNA showed an effect on sulfation of HS, CS, and *N*-glycans, whereas treatment with *PAPST2* siRNA was mainly effective on HS (Figure 5B). These results indicate that gene expression of PAPS transporters regulates sulfation in this colorectal carcinoma cell line.

Gene silencing of PAPS transporters decreases cell growth in DLD-1 cells

Cellular proliferation of the siRNA-treated cells was further analyzed. On day 8 (i.e. 1 day after the third transfection), the siRNA-treated cells were seeded onto a 96-well plate and cell growth was measured once per day for 5 days using the WST-8 assay. Cells treated with either *PAPST1* or *PAPST2* siRNA showed significantly decreased cell growth relative to the cells treated with control siRNA (Figure 6). Similar to the result of sulfation, *PAPST1* siRNA was found to have a greater effect on cell growth than *PAPST2* siRNA in the DLD-1 cells.

The cell growth of double-knockdown cells was comparable to that of *PAPST1*-single knockdown cells. These results indicate that PAPS transporters play a role in the proliferation of colorectal carcinoma cells by controlling their sulfation status.

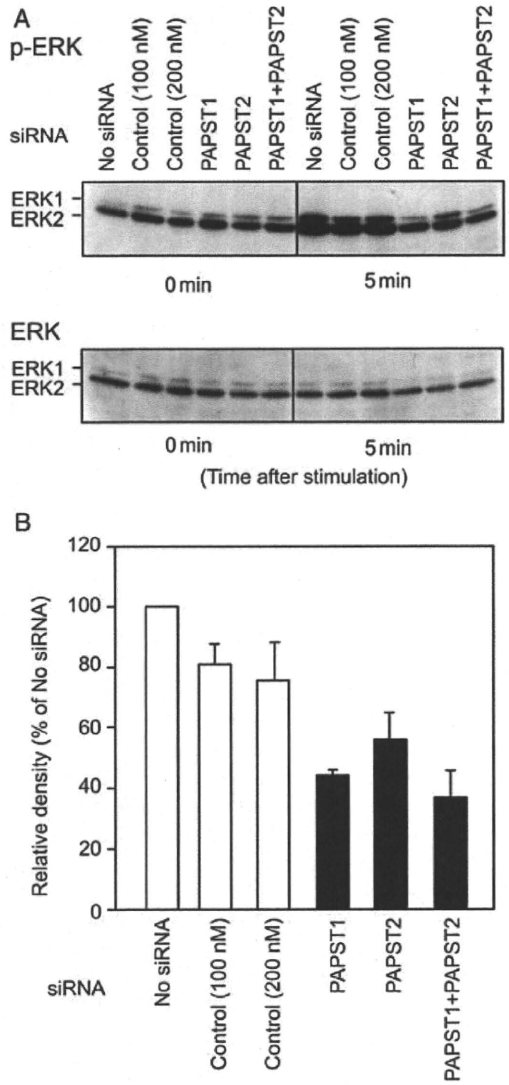

Fig. 7. FGF signaling of DLD-1 cells treated with siRNA. (**A**) Western blot analysis of ERK phosphorylation. DLD-1 cells were treated with each siRNA on days 1, 4 and 7 and stimulated with 10 ng/mL of FGF-2 on day 10. Cell lysates were prepared 0 and 5 min after stimulation and western blot analysis against ERK or phosphorylated ERK antibodies was performed. (**B**) Densitometric analysis of the western blot. Levels of phosphorylated ERK/total ERK 5 min after stimulation were calculated using the NIH Image program and the value obtained from control cells is presented as 100%. Values shown are means (SDs) obtained from three independent experiments. No siRNA, cells treated with no siRNA; control (100 nM), cells treated with 100 nM control siRNA; control (200 nM), cells treated with 200 nM control siRNA; PAPST1, cells treated with 100 nM *PAPST1* siRNA; PAPST2, cells treated with 100 nM *PAPST2* siRNA; PAPST1+PAPST2, cells treated with 100 nM *PAPST1* siRNA and 100 nM *PAPST2* siRNA.

Gene silencing of PAPS transporters reduces HS-dependent growth factor signaling in DLD-1 cells

It is known that HS is involved in many growth-factor signaling pathways with interacting growth factors. FGF-2 is one of the HS-interacting growth factors and plays a role in regulating the proliferation of cells. Because the interaction between HS and FGF-2 requires the sulfation of HS (Rapraeger et al. 1991; Yayon et al. 1991), FGF-2 signaling was analyzed in the siRNA-treated DLD-1 cells. For this experiment, the DLD-1 cells treated with each siRNA were stimulated with 10 ng/mL FGF-2 on day 10 (i.e. 3 day after the third transfection), and the transduction of FGF signaling was assessed in terms of the phosphorylation of extracellular signal-regulated kinase (ERK). Western blots of phosphorylated ERK and total ERK in the siRNA-treated cells are shown in Figure 7A. In cells treated with either *PAPST1* or *PAPST2* siRNA, the ratio of phosphorylated ERK/total ERK was decreased relative to the cells treated with control siRNA (Figure 7B). The double-knockdown cells showed the lowest value for the ERK phosphorylation. The transduction of FGF signaling reflected the sulfation status of HS in the siRNA-treated DLD-1 cells. These results indicate that the expression of PAPS transporter genes affects HS-dependent growth factor signaling in colorectal carcinoma cells.

Discussion

The present study showed that the expression level of *PAPST1* is several times higher than that of *PAPST2* in colorectal carcinoma cell lines (Figure 1A). In colorectal carcinoma tissues, the difference in expression levels of two PAPS transporters was less prominent than the difference in the cell lines (Figure 1B). Immunohistochemical analyses revealed that PAPST1 protein is predominantly expressed in epithelial cells in both noncancerous and cancerous colorectal tissues (Figure 2E–I). The expression of PAPST1 was found to be remarkably increased in fibroblasts around invasive cancer cells (Figure 2I, asterisks) but did not change in epithelial carcinoma cells of cancerous colorectal tissues. In contrast, PAPST2 protein was strongly detected in epithelial cells in noncancerous colorectal tissues (Figure 2J), whereas the expression was faintly detectable in epithelial cells in cancerous colorectal tissues (Figure 2K). Therefore, the difference in the expression levels of PAPS transporters in colorectal carcinoma cell lines might be associated with decreased *PAPST2* expression in epithelial carcinoma cells.

Several studies have reported that the composition of sulfated glycoconjugates is altered in colorectal tissues during carcinogenesis. The sialyl 6-sulfo Le^x (Izawa et al. 2000) and 3′-sulfo-Le^a (Matsushita et al. 1995; Yamachika et al. 1997) epitopes are predominantly expressed in nonmalignant colorectal tissues, but are not detected in the malignant tissues. The impaired syntheses of sialyl 6-sulfo Le^x and disialyl Le^a upon malignant transformation are responsible for the accumulation of sialyl Le^x and sialyl Le^a in colon cancer cells (Izawa et al. 2000; Kannagi 2004; Miyazaki et al. 2004). Very recently, Yusa et al. (2010) reported that diminished transcription of sulfate transporter gene *DTDST* causes decreased expression of sialyl 6-sulfo Le^x and increased expression of sialyl Le^x in colon cancer cells. Sulfate transporters and PAPS synthases are

involved in PAPS synthesis, whereas PAPS transporters are required for sulfation reaction in the Golgi apparatus. The present study showed that the expression status of PAPS transporters is also a key factor in sulfation of cellular proteins in colon cancer cells. In addition, it has been shown that several sulfotransferases exhibit altered expression levels and activities in colorectal carcinomas (Vavasseur et al. 1994; Yang et al. 1994; Kuhns et al. 1995; Seko et al. 2002a, 2002b). Further identification of alterations of sulfated glycoconjugates and components involved in sulfation during malignancy will provide valuable insights into the role of sulfation in cancer.

Silencing of PAPS transporter genes influences sulfation of proteoglycans and proliferation of colorectal carcinoma cells. Dick et al. (2008) reported that the overexpression of PAPST1 enhances the sulfation of CS in the apical pathway of MDCK cells but does not affect HS sulfation. In contrast, the present work indicates that silencing of *PAPST1* gene expression in DLD-1 cells results in a decrease in both HS and CS sulfation (Figure 5). It is known that sulfotransferases for CS have higher K_m values for PAPS than the sulfotransferases for HS (Kolset et al. 2004). The results of the present study indicate that the sulfotransferases for HS are also susceptible to the levels of substrate in the Golgi apparatus in colorectal carcinoma cells.

Silencing of PAPS transporters reduces FGF-2 signaling in DLD-1 cells. It has been reported that both HS (Rapraeger et al. 1991; Yayon et al. 1991) and CS (Deepa et al. 2002) bind to FGF-2. Because the amount of cell surface HS was found to be more than three times greater than that of cell surface CS (Figure 3), HS is considered to contribute mainly to FGF-2 signaling in DLD-1 cells. Numerous studies have shown that cell surface HS plays a crucial role in normal growth and development. It is well known that HS is required for regulation of many growth factor-signaling pathways, such as FGF (Rapraeger et al. 1991; Yayon et al. 1991), wingless/Wnt (Reichsman et al. 1996), heparin-binding, epidermal growth factor-like growth factor (Aviezer and Yayon 1994), hepatocyte growth factor (Zioncheck et al. 1995) and vascular endothelial growth factor (Soker et al. 1994; Tessler et al. 1994). We previously demonstrated that PAPS transporters are essential for normal development in *Drosophila* (Kamiyama et al. 2003; Kamiyama and Nishihara 2004; Goda et al. 2006). Lüders et al. (2003) also demonstrated that the *Drosophila* ortholog of *PAPST1* is required for signaling of wingless and hedgehog. Therefore, alteration of HS sulfation may be a significant regulatory factor for cellular proliferation in colorectal carcinomas, although the significance of CS and other glycans should also be considered. Additionally, the strong expression of PAPST1 protein in fibroblasts in the vicinity of invasive cancer cells (Figure 2I, asterisks) suggests that PAPST1 has a role in the desmoplastic reaction during tumorigenesis to support cancer growth through modulation of HS-dependent signaling.

It has been reported that the expression of nucleotide sugar transporters is altered in the case of cancer or inflammation. In these studies, it was found that the expression level of a UDP-galactose transporter (SLC35A2) is increased in human colon carcinoma and is responsible for the synthesis of Thomsen–Friedenreich antigens and sialyl Le^a and sialyl Le^x epitopes (Kumamoto et al. 2001). Expression of a GDP-fucose transporter (SLC35C1) is upregulated in hepatocellular carcinomas and plays a role in increased fucosylation (Moriwaki et al. 2007). In addition, the expression levels of transporters involved in sulfo sialyl Le^x glycan biosynthesis were coordinately upregulated by inflammation-related stimuli (Huopaniemi et al. 2004). Koike et al. (2004) reported that transcription of genes involved in the synthesis of the E-selectin ligands, namely fucosyltransferase VII, sialyltransferase ST3Gal-I and UDP-galactose transporter 1 (SLC35A2), is significantly induced in cancer cells under hypoxic culture conditions. Their study also showed that a hypoxia-inducible transcription factor induces transcription of these genes and leads to a significant increase in selectin-mediated cancer cell adhesion to endothelial cells (Koike et al. 2004). Furthermore, Yusa et al. (2010) suggested that the transcription of sulfate transporter *DTDST* is suppressed by epigenetic silencing via histone modification in colon cancer cells. It would be an interesting topic of research to elucidate how the expression of these transporter genes is transcriptionally regulated in cancer or inflammation.

Mutations in nucleotide sugar transporter genes responsible for several disorders have been recently identified (Lübke et al. 2001; Lühn et al. 2001; Martinez-Duncker et al. 2005; Hiraoka et al. 2007). With regard to the synthesis of GAGs, the mutation of a gene involved in the synthesis of CS, *SLC35D1*, was reported to be responsible for Schneckenbecken dysplasia, a severe skeletal dysplasia (Hiraoka et al. 2007). A missense mutation in the bovine *SLC35A3* gene, which encodes a UDP-*N*-acetylglucosamine transporter, causes complex vertebral malformation (Thomsen et al. 2006). To date, no disorders associated with PAPS transporter gene mutation have been reported. However, Clement et al. (2008) recently demonstrated that a zebrafish with a *PAPST1* mutation has cartilage defects that strongly resemble those seen in human patients with hereditary multiple exostoses. Additionally, analyses of *Drosophila* mutants demonstrated the significance of PAPS transporters in development (Kamiyama et al. 2003; Lüders et al. 2003; Goda et al. 2006). Our recent research has revealed that both PAPST1 and PAPST2 contribute to the maintenance and differentiation of mouse embryonic stem cells by regulating Wnt, bone morphogenetic protein and FGF signaling (Sasaki et al. 2009). The results of the present study provide additional information on the functions of PAPS transporters in cancer cells. In the future, approaches using transgenic or knockout mice would be helpful in elucidating the key roles of PAPS transporters.

Experimental procedures

Cell culture and tissue samples

Omega, DLD-1 and LS174T cell lines were cultured in Dulbecco's modified Eagle's medium (DMEM)/F12 (1:1) medium (Invitrogen Co., Carlsbad, CA), supplemented with 10% fetal bovine serum and 1× penicillin/streptomycin (Invitrogen).

The use of the clinical materials was approved by the ethical committee of the National Hospital Organization Osaka National Hospital, the Keio University Hospital, the

National Institute of Advanced Industrial Science and Technology, the Aichi Cancer Center Research Institute and Soka University. The formalin-fixed and paraffin-embedded colon cancer samples were obtained from the National Hospital Organization Osaka National Hospital and used for immunohistochemical analysis. The frozen rectal cancer samples were obtained from the Keio University Hospital and used for *in situ* hybridization. The frozen cancerous and non-cancerous colon tissues were obtained from the National Hospital Organization Osaka National Hospital and the Aichi Cancer Center Research Institute to use for quantitative PCR analysis.

Quantitative analysis of PAPST1 and PAPST2 transcripts

The quantities of *PAPST1* and *PAPST2* transcripts were determined using real-time PCR. Total RNA from human colorectal tissues was extracted using RNeasy Plus Mini (QIAGEN K.K., Tokyo, Japan) or the method of Chomczynski and Sacchi (1987). The features of each of the colorectal carcinoma samples were confirmed by histopathological examination (Table I). Total RNA from the cell lines was prepared using TRIzol reagent (Invitrogen). First-strand cDNA was synthesized with a Superscript II First Strand Synthesis kit (Invitrogen) with an oligo-dT primer. Real-time PCR was performed using qPCR Mastermix (QuickGoldStar; Eurogentec, Seraing, Belgium) and an ABI PRISM 7700 Sequence Detection System (Applied Biosystems, Foster, CA).

The PCR primer pair sequences and TaqMan probes used for each gene were same as those previously reported (Kamiyama et al. 2003, 2006). The relative amounts of *PAPST1* and *PAPST2* transcripts were normalized to the amount of glyceraldehyde 3-phosphate dehydrogenase (*GAPDH*) transcript present in the same cDNA.

In situ hybridization

A pBluescript SK(−) plasmid containing a 0.57 kb *PAPST1* sequence was linearized with *Not*I. A digoxigenin-labeled antisense riboprobe was synthesized with T7 RNA polymerase using Dig RNA Labeling Kits (Roche Applied Science, Indianapolis, IN). As a negative control, a sense riboprobe was synthesized with T3 RNA polymerase after linearization of the plasmid with *Xho*I.

Serial frozen sections prepared from rectal tissues in Tissue-Tech OCT compound (Sakura Finetechnical Co. Ltd., Tokyo, Japan) were thawed on slides and the OCT compound was removed. Sections were treated with 1 μg/mL of proteinase K at 37°C for 10 min and refixed in 4% paraformaldehyde at 4°C for 20 min. Sections were then pre-hybridized in hybridization buffer (5× SSC containing 50% deionized formamide, 10% dextran sulfate, 0.5% Tween 20, 5 mM dithiothreitol, 50 μg/mL of heparin and 50 μg/mL of yeast tRNA) and hybridized with a digoxigenin-labeled sense or antisense riboprobe in hybridization buffer at 58°C for 16 h. After hybridization, sections were sequentially washed with 5× SSC containing 50% formamide and 0.2% Tween-20 at 58°C for 30 min and three times with 2× SSC containing 50% formamide and 0.2% Tween-20 at 58°C for 30 min. The sections were then treated with 0.5% blocking buffer (Roche Applied Science) in TBST and reacted with alkaline phosphatase-conjugated anti-digoxigenin antibody (Roche Applied Science). Endogenous phosphatases were inactivated with 2 mM levamisole in TBST and riboprobes were detected with 0.375 mg/mL of nitroblue tetrazolium, 0.175 mg/mL of 5-bromo-4-chloro-3-indolyl phosphate, 100 mM NaCl, 100 mM Tris–HCl, pH 9.5, 50 mM $MgCl_2$ and 0.1% Tween-20 for 2.5 h. The developed sections were washed three times with 10 mM Tris–HCl, pH 8.0, and 1 mM EDTA and were mounted with glycerol.

Immunohistochemical analysis

Rabbit polyclonal antibodies generated against mouse PAPST1, KAVPTEPPVQKV, and human PAPST2, CAKNPVRTYGYA, were purified by using each peptide and were then used to examine the immunohistochemical distribution of PAPS transporter proteins.

For immunostaining of formalin-fixed and paraffin-embedded tissue samples, 3 μm thick sections were serially cut and mounted on precoated slides. A Ventana system (Ventana XT system BenchMark; Ventana Medical Systems, Tucson, AZ) was used for immunohistochemical analysis. All procedures were performed automatically by the system according to the manufacturer's protocols. Briefly, the tissue sections were automatically treated with an antigen-retrieval solution (Ventana) and heated on a slide heater at 100°C for 30 min. Endogenous peroxidase activity was quenched by immersion in 3% hydrogen peroxide for 4 min. The sections were then incubated with anti-PAPST1 antibody (rabbit polyclonal, 1/500 dilution) for 30 min at 37°C. Detection was performed using the LSAB Ventana Iview DAB detection system according to the manufacturer's instructions. Sections were counterstained with hematoxylin.

For immunostaining of frozen tissue sections, the sections were fixed in cold acetone for 5 min and then rehydrated in phosphate-buffered saline (PBS). The sections were incubated with a blocking reagent (5% bovine serum albumin in PBS) at room temperature for 30 min and reacted with the anti-PAPST1 antibody (rabbit polyclonal, 1:500 dilution) or the anti-PAPST2 antibody (rabbit polyclonal, 1:100 dilution) at 4°C for 16 h. After washing with PBS, the sections were incubated with anti-rabbit immunoglobulin (IgG)-conjugated Alexa Fluor 488 at room temperature for 30 min. For counter staining, the sections were treated with phallotoxins conjugated Alexa Fluor 594 (Molecular Probes, Invitrogen, Eugene, OR) to stain the F-actin for 10 min and then incubated with Hoechst 33342 to stain the nucleus for 10 min. The sections were mounted in ProLong Gold Antifade reagent (Molecular Probes).

Verification of antibody specificity

The immunoreactivity of purified anti-PAPST1 antibody to human PAPST1 protein was confirmed by western blotting. The coding region of human PAPST1 was amplified by PCR using a forward primer 5′-GAATTCTGGACGCCAGATGG TGG-3′ and a reverse primer 5′-CTCGAGTCAAACCTT CTGCACAGGAG-3′. The PCR fragment was subcloned into the *EcoR*I and *Xho*I sites of the pCXN2-c-myc vector which contains an N-terminal-c-myc tag. HEK 293 cells were subcultured onto 6 cm dishes at a concentration of 1×10^6 cells/

dish and were transfected with 2 μg of plasmid using Lipofectamine 2000 reagent (Invitrogen). Three days after the transfection, cells were suspended in 120 μL of 10 mM triethanolamine containing 0.8 M Sorbitol and lysed with 60 μL of 3× SDS sample buffer (New England Biolabs Inc., Ipswich, MA) at 4°C for 16 h. The whole cell lysate (1 μg protein) was subjected to 10% SDS–polyacrylamide gel electrophoresis (PAGE), and proteins were transferred onto polyvinylidene difluoride membranes (Millipore). The membrane blot was blocked with 5% skimmed milk in PBS containing 0.1% Tween-20 (PBST, pH 7.4) and then was immunoreacted with the anti-PAPST1 antibody (1:5000 dilution in PBST) or an anti-c-myc monoclonal antibody (1:5000 dilution in PBST; Santa Cruz Biotechnology, Inc., Santa Cruz, CA). After washing with PBST, each blot was reacted with the corresponding secondary antibody conjugated with horseradish peroxidase in PBST. The blot was washed with PBST and developed with ECL Plus reagents (GE Healthcare Bioscience, Piscataway, NJ).

Metabolic labeling and determination of total sulfate incorporation into proteins

Twenty-four hours prior to analysis, cells were subcultured in a 24-well plate at a concentration of 1×10^5 cells/well in inorganic sulfate-free DMEM/F12 medium supplemented with 10% fetal bovine serum and 100 μCi/mL of carrier-free $Na_2[^{35}S]O_4$ (American Radiolabeled Chemicals Inc., St. Louis, MO). The cells were rinsed twice with PBS, suspended in 50 μL of lysis buffer (10 mM Tris–HCl, pH 7.4, 0.5% Nonidet P-40, 1 mM EDTA and 0.5 mM phenylmethylsulfonyl fluoride) and incubated on ice for 1 h. The solution was centrifuged at 18,500 × *g* for 30 min, and the supernatant was used as the cell lysates. Twenty micrograms of the protein in each sample was precipitated with 10% TCA and washed with 5% TCA, followed by cold acetone. The precipitate was dried and dissolved in 50 μL of 0.5 N NaOH for scintillation counting.

Determination of sulfate incorporation into HS, CS and N-linked glycans

The $Na_2[^{35}S]O_4$-labeled cells were rinsed twice with PBS and cultured in normal medium for 2 h. Cells were rinsed with PBS and treated with 0.5 mL of DMEM/F12 medium containing 10 mU/mL of heparitinase (Seikagaku Kogyo, Tokyo, Japan) or 100 mU/mL of chondroitinase ABC (Seikagaku Kogyo) at 37°C for 2 h. The medium was saved and centrifuged at 18,500 × *g* for 5 min, and the supernatant was used for scintillation counting. For each sample, the value was calculated as the difference between the radioactivity obtained from cells treated with the enzyme and the background radioactivity without the enzyme.

For quantification of sulfate incorporation into *N*-linked glycans, 20 μg of protein from the cell lysate was treated with PNGase F (New England BioLabs) at 37°C for 2 h. Proteins were precipitated with 20% TCA and washed with 5% TCA, followed by cold acetone. The precipitate was dried and dissolved in 50 μL of 0.5 N NaOH for scintillation counting. The value was calculated as the difference between the radioactivity obtained from the cell lysate without the enzyme and the radioactivity from the cell lysate treated with the enzyme.

Treatment of DLD-1 cells with siRNA

Nineteen-base pair siRNAs with two bases of 3′ overhangs were designed using the siDirect program (http://genomics.jp/sidirect). The siRNA sequences used were as follows: for control siRNA, sense strand 5′-GUACCGCACGUCAUUCG UAUC-3′ and antisense strand 5′-UACGAAUGACGUGC GGUACGU-3′; for PAPST1 siRNA, sense strand 5′-GGU CAAGAGAGCAUAGGUAGG-3′ and antisense strand 5′-UA CCUAUGCUCUCUUGACCCC-3′; for PAPST2 siRNA, sense strand 5′-CCAGUUCGGACCUAUGGUUAU-3′ and antisense strand 5′-AACCAUAGGUCCGAACUGGAU-3′.

DLD-1 cells were subcultured onto 6 cm dishes at a concentration of 1×10^6 cells/dish 24 h prior to transfection. The cells were repeatedly transfected with 100 nM siRNA with Lipofectamine 2000 reagent three times on days 1, 4 and 7. On day 9, the cells were labeled with $Na_2[^{35}S]O_4$ for 24 h and analyzed as described in 'Metabolic labeling and determination of total sulfate incorporation into proteins'. RNA was extracted using TRIzol reagent (Invitrogen) on day 10.

Cell proliferation assay

Cell proliferation was assessed using an assay with a tetrazolium salt, 2-(2-methoxy-4-nitrophenyl)-3-(4-nitrophenyl)-5-(2,4-disulfophenyl)-2H tetrazolium monosodium salt (WST-8). In this experiment, cells were seeded onto a 96-well plate at a concentration of 2×10^3 cells/well in quadruplicate on day 8 and cultured in the normal medium. The number of cells was quantified once per day for 5 days using a Cell Counting Kit-8 (Dojindo Laboratories, Kumamoto, Japan). The absorbance at 450 nm was measured 2 h after the reaction using a microplate reader (Model 3550; Bio-Rad Labs, Hercules, CA). The obtained value was adjusted by subtracting the background value (obtained without the reagent).

Cell stimulation and western blot analysis

For activation of FGF signaling, cells were serum-starved for 16 h and treated with 10 ng/mL of FGF-2 (Upstate Biotechnology Inc., Lake Placid, NY) for 5 min. Cells were rinsed with ice-cold PBS and lysed in lysis buffer (50 mM Tris–HCl, pH 7.4; 150 mM NaCl, 1% Triton X-100, 1 mM Na_3VO_4, 10 mM NaF and protease inhibitors) and centrifuged at 18,500 × *g* for 5 min. The supernatant was used for western blot analysis.

For western blot analysis, proteins in the cell lysate (5 μg) were separated with 10% SDS–PAGE and transferred onto polyvinylidene difluoride membranes (Millipore). The membrane blot was blocked with 1% bovine serum albumin in 20 mM Tris-buffered saline containing 0.1% Tween-20 (TBST, pH 7.4) for 2 h at room temperature and then immunoreacted with an antibody against ERK-1/2 (Cell Signaling Technology, Beverly, MA) or phosphorylated ERK-1/2 (Thr-202 and Thr-204; Cell Signaling Technology) in blocking buffer at 4°C overnight. After washing with TBST, each blot was reacted with its corresponding secondary antibody conjugated with

horseradish peroxidase in TBST at room temperature for 1 h. The blot was washed with TBST and developed with ECL Plus reagents (GE Healthcare Bioscience).

Funding

This work was supported in part by the New Energy and Industrial Technology Development Organization (NEDO) of Japan and by the Ministry of Education, Culture, Sports, Science and Technology (MEXT) which provided a Grant-in-Aid for Scientific Research (B) to S.N., 20370051, 2008–2010, and a Matching Fund for Private Universities, S0901015, 2009–2014.

Acknowledgement

We thank Sayumi Shirakawa, M.S., for expert technical assistance.

Conflict of interest statement

None declared.

Abbreviations

CS, chondroitin sulfate; DMEM, Dulbecco's modified Eagle's medium; ERK, extracellular signal-regulated kinase; FGF, fibroblast growth factor; GAG, glycosaminoglycan; GAPDH, glyceraldehyde 3-phosphate dehydrogenase; GDP, guanidine diphosphate; HS, heparan sulfate; IgG, immunoglobulin G; Le^a, galactose β 1-3[fucose α 1-4] *N*-acetylglucosamine; Le^x, galactose β 1-4[fucose α 1-3] *N*-acetylglucosamine; PAPS, 3′-phosphoadenosine 5′-phosphosulfate; PAGE, polyacrylamide gel electrophoresis; PBS, phosphate-buffered saline; PCR, polymerase chain reaction; PBST, PBS containing 0.1% Tween-20; PNGase, peptide:*N*-glycosidase; RNAi, RNA interference; siRNA, small interfering RNA; TBST, Tris-buffered saline containing 0.1% Tween-20; TCA, trichloroacetic acid; UDP, uridine diphosphate.

References

Aviezer D, Yayon A. 1994. Heparin-dependent binding and autophosphorylation of epidermal growth factor (EGF) receptor by heparin-binding EGF-like growth factor but not by EGF. *Proc Natl Acad Sci USA.* 91:12173–12177.

Chomczynski P, Sacchi N. 1987. Single-step method of RNA isolation by acid guanidinium thiocyanate–phenol–chloroform extraction. *Anal Biochem.* 162:156–159.

Clement A, Wiweger M, von der Hardt S, Rusch MA, Selleck SB, Chien CB, Roehl HH. 2008. Regulation of zebrafish skeletogenesis by ext2/dackel and papst1/pinscher. *PLoS Genet.* 4:e1000136.

Deepa SS, Umehara Y, Higashiyama S, Itoh N, Sugahara K. 2002. Specific molecular interactions of oversulfated chondroitin sulfate E with various heparin-binding growth factors. Implications as a physiological binding partner in the brain and other tissues. *J Biol Chem.* 277:43707–43716.

Dick G, Grødahl F, Prydz K. 2008. Overexpression of the 3′-phosphoadenosine 5′-phosphosulfate (PAPS) transporter 1 increases sulfation of chondroitin sulfate in the apical pathway of MDCK II cells. *Glycobiology.* 18:53–65.

Goda E, Kamiyama S, Uno T, Yoshida H, Ueyama M, Kinoshita-Toyoda A, Toyoda H, Ueda R, Nishihara S. 2006. Identification and characterization of a novel *Drosophila* 3′-phosphoadenosine 5′-phosphosulfate transporter. *J Biol Chem.* 281:28508–28517.

Hiraoka S, Furuichi T, Nishimura G, Shibata S, Yanagishita M, Rimoin DL, Superti-Furga A, Nikkels PG, Ogawa M, Katsuyama K, et al. 2007. Nucleotide-sugar transporter SLC35D1 is critical to chondroitin sulfate synthesis in cartilage and skeletal development in mouse and human. *Nat Med.* 13:1363–1367.

Huopaniemi L, Kolmer M, Niittymaki J, Pelto-Huikko M, Renkonen R. 2004. Inflammation-induced transcriptional regulation of Golgi transporters required for the synthesis of sulfo sLex glycan epitopes. *Glycobiology.* 14:1285–1294.

Irimura T, Wynn DM, Hager LG, Cleary KR, Ota DM. 1991. Human colonic sulfomucin identified by a specific monoclonal antibody. *Cancer Res.* 51:5728–5735.

Izawa M, Kumamoto K, Mitsuoka C, Kanamori C, Kanamori A, Ohmori K, Ishida H, Nakamura S, Kurata-Miura K, Sasaki K, et al. 2000. Expression of sialyl 6-sulfo Lewis X is inversely correlated with conventional sialyl Lewis X expression in human colorectal cancer. *Cancer Res.* 60:1410–1416.

Kamimura K, Fujise M, Villa F, Izumi S, Habuchi H, Kimata K, Nakato H. 2001. *Drosophila* heparan sulfate 6-*O*-sulfotransferase (*dHS6ST*) gene. Structure, expression, and function in the formation of the tracheal system. *J Biol Chem.* 276:17014–17021.

Kamimura K, Koyama T, Habuchi H, Ueda R, Masu M, Kimata K, Nakato H. 2006. Specific and flexible roles of heparan sulfate modifications in *Drosophila* FGF signaling. *J Cell Biol.* 174:773–778.

Kamiyama S, Nishihara S. 2004. The subcellular PAPS synthesis pathway responsible for the sulfation of proteoglycans: A comparison between humans and *Drosophila melanogaster*. *Trends Glycosci Glycotechnol.* 16:109–123.

Kamiyama S, Sasaki N, Goda E, Ui-Tei K, Saigo K, Narimatsu H, Jigami Y, Kannagi R, Irimura T, Nishihara S. 2006. Molecular cloning and characterization of a novel 3′-phosphoadenosine 5′-phosphosulfate transporter, PAPST2. *J Biol Chem.* 281:10945–10953.

Kamiyama S, Suda T, Ueda R, Suzuki M, Okubo R, Kikuchi N, Chiba Y, Goto S, Toyoda H, Saigo K, et al. 2003. Molecular cloning and identification of 3′-phosphoadenosine 5′-phosphosulfate transporter. *J Biol Chem.* 278:25958–25963.

Kannagi R. 2004. Molecular mechanism for cancer-associated induction of sialyl Lewis X and sialyl Lewis A expression—the Warburg effect revisited. *Glycoconj J.* 20:353–364.

Koike T, Kimura N, Miyazaki K, Yabuta T, Kumamoto K, Takenoshita S, Chen J, Kobayashi M, Hosokawa M, Taniguchi A, et al. 2004. Hypoxia induces adhesion molecules on cancer cells: A missing link between Warburg effect and induction of selectin-ligand carbohydrates. *Proc Natl Acad Sci USA.* 101:8132–8137.

Kolset SO, Prydz K, Pejler G. 2004. Intracellular proteoglycans. *Biochem J.* 379:217–227.

Kuhns W, Jain RK, Matta KL, Paulsen H, Baker MA, Geyer R, Brockhausen I. 1995. Characterization of a novel mucin sulphotransferase activity synthesizing sulphated *O*-glycan core 1,3-sulphate-Gal β 1-3GalNAc α-R. *Glycobiology.* 5:689–697.

Kumamoto K, Goto Y, Sekikawa K, Takenoshita S, Ishida N, Kawakita M, Kannagi R. 2001. Increased expression of UDP-galactose transporter messenger RNA in human colon cancer tissues and its implication in synthesis of Thomsen-Friedenreich antigen and sialyl Lewis A/X determinants. *Cancer Res.* 61:4620–4627.

Lin X, Buff EM, Perrimon N, Michelson AM. 1999. Heparan sulfate proteoglycans are essential for FGF receptor signaling during *Drosophila* embryonic development. *Development.* 126:3715–3723.

Lin X, Perrimon N. 1999. Dally cooperates with *Drosophila* Frizzled 2 to transduce Wingless signalling. *Nature.* 400:281–284.

Lübke T, Marquardt T, Etzioni A, Hartmann E, von Figura K, Körner C. 2001. Complementation cloning identifies CDG-IIc, a new type of congenital disorders of glycosylation, as a GDP-fucose transporter deficiency. *Nat Genet.* 28:73–76.

Lüders F, Segawa H, Stein D, Selva EM, Perrimon N, Turco SJ, Häcker U. 2003. *Slalom* encodes an adenosine 3′-phosphate 5′-phosphosulfate transporter essential for development in *Drosophila*. *EMBO J.* 22:3635–3644.

Lühn K, Wild MK, Eckhardt M, Gerardy-Schahn R, Vestweber D. 2001. The gene defective in leukocyte adhesion deficiency II encodes a putative GDP-fucose transporter. *Nat Genet.* 28:69–72.

Martinez-Duncker I, Dupre T, Piller V, Piller F, Candelier JJ, Trichet C, Tchernia G, Oriol R, Mollicone R. 2005. Genetic complementation reveals

a novel human congenital disorder of glycosylation of type II, due to inactivation of the Golgi CMP-sialic acid transporter. *Blood.* 105:2671–2676.

Matsushita Y, Yamamoto N, Shirahama H, Tanaka S, Yonezawa S, Yamori T, Irimura T, Sato E. 1995. Expression of sulfomucins in normal mucosae, colorectal adenocarcinomas, and metastases. *Jpn J Cancer Res.* 86:1060–1067.

Mitsuoka C, Sawada-Kasugai M, Ando-Furui K, Izawa M, Nakanishi H, Nakamura S, Ishida H, Kiso M, Kannagi R. 1998. Identification of a major carbohydrate capping group of the L-selectin ligand on high endothelial venules in human lymph nodes as 6-sulfo sialyl Lewis X. *J Biol Chem.* 273:11225–11233.

Miyazaki K, Ohmori K, Izawa M, Koike T, Kumamoto K, Furukawa K, Ando T, Kiso M, Yamaji T, Hashimoto Y, et al. 2004. Loss of disialyl Lewis(a), the ligand for lymphocyte inhibitory receptor sialic acid-binding immunoglobulin-like lectin-7 (Siglec-7) associated with increased sialyl Lewis(a) expression on human colon cancers. *Cancer Res.* 64:4498–4505.

Moriwaki K, Noda K, Nakagawa T, Asahi M, Yoshihara H, Taniguchi N, Hayashi N, Miyoshi E. 2007. A high expression of GDP-fucose transporter in hepatocellular carcinoma is a key factor for increases in fucosylation. *Glycobiology.* 17:1311–1320.

Nakamori S, Kameyama M, Imaoka S, Furukawa H, Ishikawa O, Sasaki Y, Kabuto T, Iwanaga T, Matsushita Y, Irimura T. 1993. Increased expression of sialyl Lewisx antigen correlates with poor survival in patients with colorectal carcinoma: Clinicopathological and immunohistochemical study. *Cancer Res.* 53:3632–3637.

Nakayama T, Watanabe M, Katsumata T, Teramoto T, Kitajima M. 1995. Expression of sialyl Lewis(a) as a new prognostic factor for patients with advanced colorectal carcinoma. *Cancer.* 75:2051–2056.

Rapraeger AC, Krufka A, Olwin BB. 1991. Requirement of heparan sulfate for bFGF-mediated fibroblast growth and myoblast differentiation. *Science.* 252:1705–1708.

Reichsman F, Smith L, Cumberledge S. 1996. Glycosaminoglycans can modulate extracellular localization of the wingless protein and promote signal transduction. *J Cell Biol.* 135:819–827.

Sasaki N, Hirano T, Ichimiya T, Wakao M, Hirano K, Kinoshita-Toyoda A, Toyoda H, Suda Y, Nishihara S. 2009. The 3′-phosphoadenosine 5′-phosphosulfate transporters, PAPST1 and 2, contribute to the maintenance and differentiation of mouse embryonic stem cells. *PLoS ONE.* 4: e8262.

Seko A, Nagata K, Yonezawa S, Yamashita K. 2002a. Ectopic expression of a GlcNAc 6-*O*-sulfotransferase, GlcNAc6ST-2, in colonic mucinous adenocarcinoma. *Glycobiology.* 12:379–388.

Seko A, Nagata K, Yonezawa S, Yamashita K. 2002b. Down-regulation of Gal 3-*O*-sulfotransferase-2 (Gal3ST-2) expression in human colonic nonmucinous adenocarcinoma. *Jpn J Cancer Res.* 93:507–515.

Soker S, Goldstaub D, Svahn CM, Vlodavsky I, Levi BZ, Neufeld G. 1994. Variations in the size and sulfation of heparin modulate the effect of heparin on the binding of VEGF165 to its receptors. *Biochem Biophys Res Commun.* 203:1339–1347.

Tessler S, Rockwell P, Hicklin D, Cohen T, Levi BZ, Witte L, Lemischka IR, Neufeld G. 1994. Heparin modulates the interaction of VEGF165 with soluble and cell associated flk-1 receptors. *J Biol Chem.* 269: 12456–12461.

Thomsen B, Horn P, Panitz F, Bendixen E, Petersen AH, Holm LE, Nielsen VH, Agerholm JS, Arnbjerg J, Bendixen C. 2006. A missense mutation in the bovine *SLC35A3* gene, encoding a UDP-*N*-acetylglucosamine transporter, causes complex vertebral malformation. *Genome Res.* 16:97–105.

Tsuiji H, Hayashi M, Wynn DM, Irimura T. 1998a. Expression of mucin-associated sulfo-Lea carbohydrate epitopes on human colon carcinoma cells. *Jpn J Cancer Res.* 89:1267–1275.

Tsuiji H, Hong JC, Kim YS, Ikehara Y, Narimatsu H, Irimura T. 1998b. Novel carbohydrate specificity of monoclonal antibody 91.9H prepared against human colonic sulfomucin: Recognition of sulfo-Lewis(a) structure. *Biochem Biophys Res Commun.* 253:374–381.

Vavasseur F, Dole K, Yang J, Matta KL, Myerscough N, Corfield A, Paraskeva C, Brockhausen I. 1994. *O*-glycan biosynthesis in human colorectal adenoma cells during progression to cancer. *Eur J Biochem.* 222:415–424.

Yamachika T, Nakanishi H, Inada K, Kitoh K, Kato T, Irimura T, Tatematsu M. 1997. Reciprocal control of colon-specific sulfomucin and sialosyl-Tn antigen expression in human colorectal neoplasia. *Virchows Arch.* 431:25–30.

Yamori T, Ota DM, Cleary KR, Hoff S, Hager LG, Irimura T. 1989. Monoclonal antibody against human colonic sulfomucin: Immunochemical detection of its binding sites in colonic mucosa, colorectal primary carcinoma, and metastases. *Cancer Res.* 49:887–894.

Yang JM, Byrd JC, Siddiki BB, Chung YS, Okuno M, Sowa M, Kim YS, Matta KL, Brockhausen I. 1994. Alterations of *O*-glycan biosynthesis in human colon cancer tissues. *Glycobiology.* 4:873–884.

Yayon A, Klagsbrun M, Esko JD, Leder P, Ornitz DM. 1991. Cell surface, heparin-like molecules are required for binding of basic fibroblast growth factor to its high affinity receptor. *Cell.* 64:841–848.

Yusa A, Miyazaki K, Kimura N, Izawa M, Kannagi R. 2010. Epigenetic silencing of the sulfate transporter gene *DTDST* induces sialyl Lewisx expression and accelerates proliferation of colon cancer cells. *Cancer Res.* 70:4064–4073.

Zioncheck TF, Richardson L, Liu J, Chang L, King KL, Bennett GL, Fugedi P, Chamow SM, Schwall RH, Stack RJ. 1995. Sulfated oligosaccharides promote hepatocyte growth factor association and govern its mitogenic activity. *J Biol Chem.* 270:16871–16878.